

# QUANTUM GRAVITY AT ASTROPHYSICAL DISTANCES?

M. Reuter and H. Weyer

*Institute of Physics, University of Mainz  
Staudingerweg 7, D-55099 Mainz, Germany*

## Abstract

Assuming that Quantum Einstein Gravity (QEG) is the correct theory of gravity on all length scales we use analytical results from nonperturbative renormalization group (RG) equations as well as experimental input in order to characterize the special RG trajectory of QEG which is realized in Nature and to determine its parameters. On this trajectory, we identify a regime of scales where gravitational physics is well described by classical General Relativity. Strong renormalization effects occur at both larger and smaller momentum scales. The latter lead to a growth of Newton's constant at large distances. We argue that this effect becomes visible at the scale of galaxies and could provide a solution to the astrophysical missing mass problem which does not require any dark matter. We show that an extremely weak power law running of Newton's constant leads to flat galaxy rotation curves similar to those observed in Nature. Furthermore, a possible resolution of the cosmological constant problem is proposed by noting that all RG trajectories admitting a long classical regime automatically give rise to a small cosmological constant.

# 1 Introduction

During the past few years, in the light of a series of investigations [1–9], it appeared increasingly likely that Quantum Einstein Gravity (QEG), the quantum field theory of gravity whose underlying degrees of freedom are those of the spacetime metric, can be defined nonperturbatively as a fundamental, “asymptotically safe” [10] theory. By definition, its bare action is given by a non–Gaussian renormalization group (RG) fixed point. In the framework of the effective average action [11–13] a suitable fixed point is known to exist in the Einstein–Hilbert truncation of theory space [1, 3, 6] and a higher–derivative generalization [5] thereof. Detailed analyses of the reliability of this approximation [3–5] and a conceptually independent investigation [14] suggest that the fixed point should indeed exist in the exact theory, implying its nonperturbative renormalizability.

The general picture regarding the RG behavior of QEG as it has emerged so far points towards a certain analogy between QEG and non–Abelian Yang–Mills theories, Quantum Chromo–Dynamics (QCD) say. For example, like the Yang–Mills coupling constant, the running Newton constant  $G = G(k)$  is an asymptotically free coupling, it vanishes in the ultraviolet (UV), i. e. when the typical momentum scale  $k$  becomes large. In QCD the realm of asymptotic freedom, probed in deep inelastic scattering processes, for instance, is realized for momenta  $k$  larger than the mass scale  $\Lambda_{\text{QCD}}$  which is induced dynamically by dimensional transmutation. In QEG the analogous role is played by the Planck mass  $m_{\text{Pl}}$ . It delimits the asymptotic scaling region towards the infrared (IR). For  $k \gg m_{\text{Pl}}$  the RG flow is well described by its linearization about the non–Gaussian fixed point [4]. Both in QCD and QEG simple local truncations of the running Wilsonian action (effective average action) are sufficient above  $\Lambda_{\text{QCD}}$  and  $m_{\text{Pl}}$ , respectively. However, as the scale  $k$  approaches  $\Lambda_{\text{QCD}}$  or  $m_{\text{Pl}}$  from above, many complicated, typically nonlocal terms are generated in the effective action [8, 15, 16]. In fact, in the IR, strong renormalization effects are to be expected because gauge (diffeomorphism) invariance leads to a massless excitation, the gluon (graviton), implying potential IR divergences which the RG flow must cure in a dynamical way. Because of the enormous algebraic complexity of the corresponding flow equations it is extremely difficult to explore the RG flow of QCD or QEG in the IR, far below the UV scaling regime, by purely analytical methods. In QCD lattice techniques can be used to study the IR sector, but despite recent progress on

dynamical triangulations [17,18] there exists no comparable tool for gravity yet.

In QCD we have another source of information about its small momentum or large distance regime. If we take it for granted that QCD is the correct theory we can exploit the available experimental data on the strong interaction, interpret them within this theory, and thus obtain information about the quantum dynamics of QCD, in particular its nonperturbative IR sector, from the purely phenomenological side. An example to which we shall come back in a moment are the non-relativistic quark-antiquark potentials extracted from quarkonium data (and confirmed on the lattice). They suggest that nonperturbative IR effects modify the classical Coulomb term by adding a confinement potential to it which increases (linearly) with distance:

$$V(r) = -\frac{a}{r} + \kappa r. \tag{1}$$

Here  $a$  and the string tension  $\kappa$  are constants [19].

In this paper we are going to apply a similar “phenomenological” strategy to gravity. Under the assumption that QEG is the correct theory of gravity on all distance scales, we try to describe and characterize the distinguished RG trajectory which is realized in Nature as completely as possible. We use both observational input and the available analytical RG studies.

We shall start from the flow equations in the Einstein–Hilbert truncation, determine which type of its RG trajectories the one realized in Nature belongs to, identify a regime on it where standard General Relativity is valid, and finally argue that this regime does not extend to arbitrarily large distances. In fact, for  $k$  smaller than the momenta typical of the regime of standard gravity, the truncation predicts a strong increase of  $G(k)$  with decreasing  $k$ , which, at a certain critical value of  $k$ , becomes infinite even. The diverging behavior is clearly an artifact of an insufficient truncation, but we shall see that the growth of Newton’s constant with the distance can be understood on general grounds as due to a potential IR singularity. It is the main hypothesis of the present paper that a “tamed” form of this nonperturbative IR growth of  $G(k)$  is a genuine feature of exact QEG.<sup>1</sup>

The problem of the missing mass or “dark matter” is one of the most puzzling mysteries of modern astrophysics and cosmology [24]. It has been known for a long time

---

<sup>1</sup>Using different methods or models, IR quantum gravity effects have also been studied in refs. [20–23].

that the luminous matter contained in a galaxy, for instance, does not provide enough mass to explain the gravitational pull the galaxy exerts on “test masses” in its vicinity. Typically their rotation curves  $v(r)$ , the orbital velocity as a function of the distance, are almost flat at large distances rather than fall off according to Kepler’s law [25]. Similar, but even stronger mass discrepancies are observed on all larger distance scales and in particular in cosmology. The recent high–redshift supernova and CMBR data show very impressively that the known forms of baryonic matter account only for a small percentage of the matter in the Universe. A possible way out is the assumption that the missing mass is due to some sort of “dark matter” which would manifest itself only by its gravitational effects. However, as to yet it has not been possible to convincingly identify any dark matter candidate, and so it might be worthwhile to think about alternatives.

It is a very intriguing idea that the apparent mass discrepancy is not due to an unknown form of matter we have not discovered yet but rather indicates that we are using the wrong theory of gravity, Newton’s law in the non–relativistic and General Relativity in the relativistic case. In fact, Milgrom [26] has developed a phenomenologically very successful non–relativistic theory, called M<sup>O</sup>modified Newtonian Dynamics or “MOND”, which explains many properties of galaxies, in particular their rotation curves, in a unified way without invoking any dark matter. In its version where gravity (rather than inertia) is modified, a point mass  $M$  produces the potential

$$\phi(r) = -\frac{\bar{G}M}{r} + \sqrt{a_0 \bar{G}M} \ln(r) \quad (2)$$

where  $\bar{G}$  and  $a_0$  are constants. The second term on the RHS of (2) is responsible for the flat, non–Keplerian rotation curves at large distances. So far no wholly satisfactory relativistic extension of MOND is known.

Also the relativistic theory proposed by Mannheim [27] where the Lagrangian is the square of the Weyl tensor tries to explain the rotation curves as due to a non–Newtonian force. The corresponding potential is of the form

$$\phi(r) = -\frac{\bar{G}M}{r} + \tilde{\kappa} r. \quad (3)$$

The resulting rotation curves do not become flat but still seem to be in accord with the observations.

For a detailed discussion of other attempts at modifying gravity at astrophysical distances and a comprehensive list of references we refer to [28]. A possible relation to quintessence has been speculated about in [29].

In the present paper we are going to explore the idea that the IR quantum effects of QEG, in particular the growth of  $G$  at large distances, induces a modified Newtonian potential similar to (2) or (3). If so, one can perhaps solve the missing mass problem in a very elegant and “minimal” manner by simply quantizing the fields which are known to exist anyhow, without having to introduce “dark matter” on an ad hoc basis.<sup>2</sup>

It is particularly intriguing that the potentials we would like to derive within QEG are strikingly similar to the nonperturbative quark–antiquark potentials generated by (quenched) QCD. In particular eqs. (1) and (3) are mathematically identical, describing “linear confinement”, while the MOND potential increases slightly more slowly at large distances. In view of the many similarities between QCD and QEG it is hard to believe that this should be a mere coincidence.

The purpose of the present paper is to learn as much as possible about the gravitational RG trajectory Nature has chosen and to investigate the possibility that the IR renormalization effects of QEG are “at work” at galactic and cosmological scales.

The remaining sections of the paper are organized as follows. In Section 2 we discuss the Einstein–Hilbert truncation of theory space with an emphasis on the strong IR renormalization effects it gives rise to. In Sections 3 and 4, we analyze the RG trajectory realized in Nature, first using mostly analytical results (Section 3) and then also phenomenological input (Section 4). In Section 5 we employ a plausible model of the trajectory in the deep IR to demonstrate that an extremely tiny variation of Newton’s constant would explain the observed flat rotation curves. The results are summarized in Section 6.

---

<sup>2</sup>See refs. [22,23] for a related analysis within a perturbatively renormalizable higher derivative gravity.

## 2 Towards the infrared with the Einstein–Hilbert truncation

In this section we discuss some properties of the Einstein–Hilbert truncation, in particular the classification of its RG trajectories. The emphasis will be on their behavior in the IR. We refer to [1] and [4] for further details.

Our basic tool is the effective average action  $\Gamma_k[g_{\mu\nu}]$ , a free energy functional which depends on the metric and a momentum scale  $k$  with the interpretation of a variable infrared cutoff. The action  $\Gamma_k$  is similar to the ordinary effective action  $\Gamma$  which it approaches for  $k \rightarrow 0$ . The main difference is that the path integral defining  $\Gamma_k$  extends only over quantum fluctuations with covariant momenta  $p^2 > k^2$ . The modes with  $p^2 < k^2$  are given a momentum dependent (mass)<sup>2</sup>  $\propto R_k(p^2)$  and are suppressed therefore. As a result,  $\Gamma_k$  describes the dynamics of metrics averaged over spacetime volumes of linear dimension  $k^{-1}$ . The functional  $\Gamma_k[g_{\mu\nu}]$  gives rise to an effective field theory valid near the scale  $k$ . Hence, when evaluated at tree level,  $\Gamma_k$  correctly describes all quantum gravitational phenomena, including all loop effects, provided the typical momentum scales involved are all of order  $k$ .

Considered a function of  $k$ ,  $\Gamma_k$  describes a RG trajectory in the space of all action functionals. The trajectory can be obtained by solving an exact functional RG equation. In practice one has to resort to approximations. Nonperturbative approximate solutions can be obtained by truncating the space of action functionals, i. e. by projecting the RG flow onto a finite–dimensional subspace which encapsulates the essential physics.

The “Einstein–Hilbert truncation”, for instance, approximates  $\Gamma_k$  by a linear combination of the monomials  $\int\sqrt{g} R$  and  $\int\sqrt{g}$ . Their prefactors contain the running Newton constant  $G(k)$  and the running cosmological constant  $\Lambda(k)$ . Their  $k$ –dependence is governed by a system of two coupled ordinary differential equations.

The flow equations resulting from the Einstein–Hilbert truncation are most conveniently written down in terms of the dimensionless “couplings”  $g(k) \equiv k^{d-2} G(k)$  and  $\lambda(k) \equiv \Lambda(k)/k^2$  where  $d$  is the dimensionality of spacetime. Parameterizing the RG trajectories by the “RG time”  $t \equiv \ln k$  the coupled system of differential equations for  $g$  and

$\lambda$  reads  $\partial_t \lambda = \beta_\lambda$ ,  $\partial_t g = \beta_g$ , where the  $\beta$ -functions are given by

$$\begin{aligned} \beta_\lambda(\lambda, g) = & -(2 - \eta_N) \lambda + \frac{1}{2} (4\pi)^{1-d/2} g \\ & \times \left[ 2 d(d+1) \Phi_{d/2}^1(-2\lambda) - 8 d \Phi_{d/2}^1(0) - d(d+1) \eta_N \tilde{\Phi}_{d/2}^1(-2\lambda) \right] \end{aligned} \quad (4)$$

$$\beta_g(\lambda, g) = (d - 2 + \eta_N) g$$

Here  $\eta_N$ , the anomalous dimension of the operator  $\int \sqrt{g} R$ , has the representation

$$\eta_N(g, \lambda) = \frac{g B_1(\lambda)}{1 - g B_2(\lambda)}. \quad (5)$$

The functions  $B_1(\lambda)$  and  $B_2(\lambda)$  are defined by

$$\begin{aligned} B_1(\lambda) \equiv & \frac{1}{3} (4\pi)^{1-d/2} \left[ d(d+1) \Phi_{d/2-1}^1(-2\lambda) - 6 d(d-1) \Phi_{d/2}^2(-2\lambda) \right. \\ & \left. - 4 d \Phi_{d/2-1}^1(0) - 24 \Phi_{d/2}^2(0) \right] \end{aligned} \quad (6)$$

$$B_2(\lambda) \equiv -\frac{1}{6} (4\pi)^{1-d/2} \left[ d(d+1) \tilde{\Phi}_{d/2-1}^1(-2\lambda) - 6 d(d-1) \tilde{\Phi}_{d/2}^2(-2\lambda) \right].$$

The above expressions contain the ‘‘threshold functions’’  $\Phi_n^p$  and  $\tilde{\Phi}_n^p$ . They are given by

$$\Phi_n^p(w) = \frac{1}{\Gamma(n)} \int_0^\infty dz z^{n-1} \frac{R^{(0)}(z) - z R^{(0)'}(z)}{[z + R^{(0)}(z) + w]^p} \quad (7)$$

and a similar formula for  $\tilde{\Phi}_n^p$  without the  $R^{(0)'}$ -term. In fact,  $R^{(0)}$  is a dimensionless version of the cutoff function  $R_k$ , i. e.  $R_k(p^2) \propto k^2 R^{(0)}(p^2/k^2)$ . Eq. (7) shows that  $\Phi_n^p(w)$  becomes singular for  $w \rightarrow -1$ . (For all admissible cutoffs,  $z + R^{(0)}(z)$  assumes its minimum value 1 at  $z = 0$  and increases monotonically for  $z > 0$ .) If  $\lambda > 0$ , the  $\Phi$ 's in the  $\beta$ -functions are evaluated at negative arguments  $w \equiv -2\lambda$ . As a result, the  $\beta$ -functions diverge for  $\lambda \nearrow 1/2$  and the RG equations define a flow on a half-plane only:  $-\infty < g < \infty$ ,  $-\infty < \lambda < 1/2$ .

This point becomes particularly clear if one uses a sharp cutoff [4]. Then the  $\Phi$ 's either display a pole at  $w = -1$ ,

$$\Phi_n^p(w) = \frac{1}{\Gamma(n)} \frac{1}{p-1} \frac{1}{(1+w)^{p-1}} \quad \text{for } p > 1, \quad (8)$$

or, in the special case  $p = 1$ , they have a logarithmic singularity at  $w = -1$ :

$$\Phi_n^1(w) = -\Gamma(n)^{-1} \ln(1+w) + \varphi_n. \quad (9)$$

The constants  $\varphi_n \equiv \Phi_n^1(0)$  parameterize the residual cutoff scheme dependence which is still present after having opted for a sharp cutoff. In numerical calculations we shall take them equal to the corresponding  $\Phi_n^1(0)$ -value of a smooth exponential cutoff<sup>3</sup>, but their precise value has no influence on the qualitative features of the RG flow [4]. The corresponding  $\tilde{\Phi}$ 's are constant for the sharp cutoff:  $\tilde{\Phi}_n^1(w) = \delta_{p1}/\Gamma(n+1)$ .

From now on we continue the discussion in  $d = 4$  dimensions. Then, with the sharp cutoff, the coupled RG equations assume the following form:

$$\partial_t \lambda = -(2 - \eta_N) \lambda - \frac{g}{\pi} \left[ 5 \ln(1 - 2\lambda) - \varphi_2 + \frac{5}{4} \eta_N \right] \quad (10a)$$

$$\partial_t g = (2 + \eta_N) g \quad (10b)$$

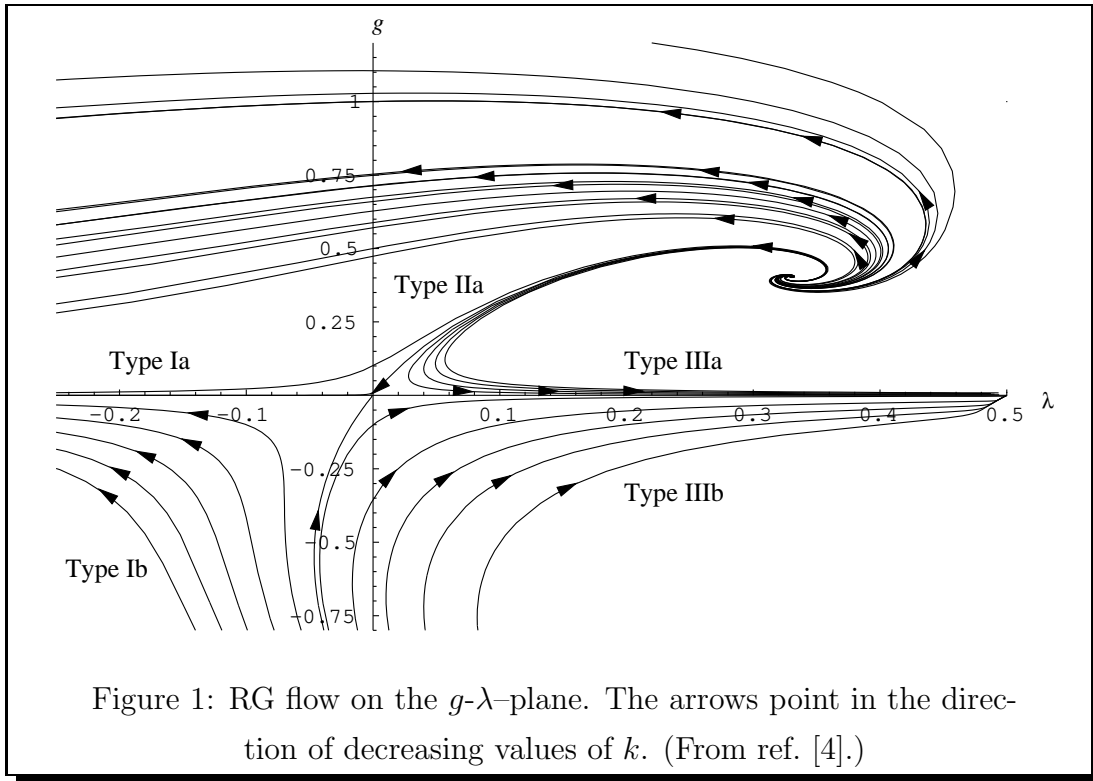
$$\eta_N = -\frac{2g}{6\pi + 5g} \left[ \frac{18}{1 - 2\lambda} + 5 \ln(1 - 2\lambda) - \varphi_1 + 6 \right]. \quad (10c)$$

Solving the system (10) numerically [4] we obtain the phase portrait shown in Fig. 1. The RG flow is dominated by two fixed points  $(g_*, \lambda_*)$ : a Gaussian fixed point (GFP) at  $g_* = \lambda_* = 0$ , and a non-Gaussian fixed point (NGFP) with  $g_* > 0$  and  $\lambda_* > 0$ . There are three classes of trajectories emanating from the NGFP: trajectories of Type Ia and IIIa run towards negative and positive cosmological constants, respectively, and the single trajectory of Type IIa (“separatrix”) hits the GFP for  $k \rightarrow 0$ . The short-distance properties of QEG are governed by the NGFP; for  $k \rightarrow \infty$ , in Fig. 1 all RG trajectories on the half-plane  $g > 0$  run into this point. The conjectured nonperturbative renormalizability of QEG is due to the NGFP: if it is present in the full RG equations, it can be used to construct a microscopic quantum theory of gravity by taking the limit of infinite UV cutoff along one of the trajectories running into the NGFP, thus being sure that the theory does not develop uncontrolled singularities at high energies [10]. By definition, QEG is the theory whose bare action  $S$  equals the fixed point action  $\lim_{k \rightarrow \infty} \Gamma_k[g_{\mu\nu}]$ .

The trajectories of Type IIIa have an important property which is not resolved in Fig. 1. Within the Einstein–Hilbert approximation they cannot be continued all the way

---

<sup>3</sup>For this purpose we employ the exponential cutoff with “shape parameter”  $s = 1$ . In  $d = 4$ , the only  $\varphi$ 's we need are  $\varphi_1 = \zeta(2)$  and  $\varphi_2 = 2\zeta(3)$ . See ref. [4] for a detailed discussion of the sharp cutoff.



down to the infrared ( $k = 0$ ) but rather terminate at a finite scale  $k_{\text{term}} > 0$ . At this scale they hit the singular boundary  $\lambda = 1/2$  where the  $\beta$ -functions diverge. As a result, the flow equations cannot be integrated beyond this point. The value of  $k_{\text{term}}$  depends on the trajectory considered.

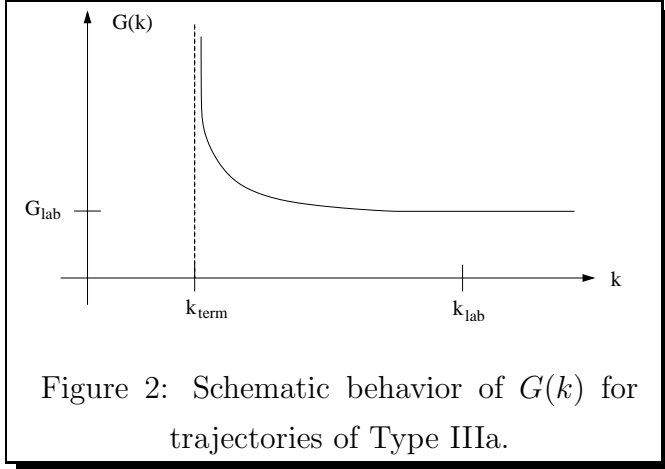
In ref. [4] the behavior of  $g$  and  $\lambda$  close to the boundary was studied in detail. The aspect which is most interesting for the present discussion is the following. As the trajectory gets close to the boundary,  $\lambda$  approaches  $1/2$  from below. In this domain the anomalous dimension (10c) is dominated by its pole term:

$$\eta_N \approx -\frac{36g}{6\pi + 5g} \frac{1}{1 - 2\lambda}. \quad (11)$$

Obviously  $\eta_N \searrow -\infty$  for  $\lambda \nearrow 1/2$ , and eventually  $\eta_N = -\infty$  at the boundary. This behavior has a dramatic consequence for the (dimensionful) Newton constant. Since  $\partial_t G = \eta_N G$ , the large and negative anomalous dimension causes  $G$  to grow very strongly when  $k$  approaches  $k_{\text{term}}$  from above. This behavior is sketched schematically in Fig. 2.

At moderately large scales  $k$ , well below the NGFP regime,  $G$  is approximately constant. As  $k$  is lowered towards  $k_{\text{term}}$ ,  $G(k)$  starts growing because of the pole in  $n_N \propto$

$1/(1 - 2\lambda)$ , and finally, at  $k = k_{\text{term}}$ , it develops a vertical tangent,  $(dG/dk)(k_{\text{term}}) = -\infty$ . The cosmological constant is finite at the termination point:  $\Lambda(k_{\text{term}}) = k_{\text{term}}^2/2$ .



By fine-tuning the parameters of the trajectory the scale  $k_{\text{term}}$  can be made as small as we like.

Since it happens only very close to  $\lambda = 1/2$ , the divergence at  $k_{\text{term}}$  is not visible on the scale of Fig. 1. (Note also that  $g$  and  $G$  are related by a decreasing factor of  $k^2$ .)

The phenomenon of trajectories which terminate at a finite scale is not special to gravity, it occurs also in truncated flow equations of theories which are understood much better. Typically it is a symptom which indicates that the truncation used becomes insufficient at small  $k$ . In QCD, for instance, thanks to asymptotic freedom, simple local truncations are sufficient in the UV, but a reliable description in the IR requires many complicated (nonlocal) terms in the truncation ansatz. Thus the conclusion is that for trajectories of Type IIIa the Einstein–Hilbert truncation is reliable only well above  $k_{\text{term}}$ . It is to be expected, though, that in an improved truncation those trajectories can be continued to  $k = 0$ .

We believe that while the Type IIIa trajectories of the Einstein–Hilbert truncation become unreliable very close to  $k_{\text{term}}$ , their prediction of a growing  $G(k)$  for decreasing  $k$  in the IR is actually correct. The function  $G(k)$  obtained from the differential equations (10) should be reliable, at least at a qualitative level, as long as  $\lambda \ll 1$ . For special trajectories the IR growth of  $G(k)$  sets in at extremely small scales  $k$  only. Later on we shall argue on the basis of a gravitational “RG improvement” [30–35] that this IR growth is responsible for the non–Keplerian rotation curves observed in spiral galaxies.

The other trajectories with  $g > 0$ , the Types Ia and IIa, do not terminate at a finite scale. The analysis of ref. [4] suggests that they are reliably described by the Einstein–

Hilbert truncation all the way down to  $k = 0$ .

We close this section with another instructive look at the phenomenon of the terminating Type IIIa trajectories. It is related to an infrared instability which is easily understood in general terms. In a slightly symbolic notation the exact RG equation for the effective average action reads [11, 12]

$$\partial_t \Gamma_k = \frac{1}{2} \text{Tr} \left[ (\Gamma_k^{(2)} + R_k)^{-1} \partial_t R_k \right]. \quad (12)$$

It contains the fully dressed effective propagator  $(\Gamma_k^{(2)} + R_k)^{-1}$  where  $\Gamma_k^{(2)}$  denotes the Hessian of  $\Gamma_k$  and  $R_k$  the cutoff operator. Upon projecting the RG flow onto the Einstein–Hilbert truncation subspace this propagator assumes the concrete form

$$\left[ -D^2 + k^2 R^{(0)} \left( -D^2/k^2 \right) - 2 \Lambda(k) \right]^{-1}. \quad (13)$$

Here  $D^2$  is the covariant Laplacian, and the trace in (12) is a sum over its eigenvalues  $-p^2$ ,  $p^2 > 0$ . In the eigenbasis the denominator of (13) becomes  $p^2 + k^2 R^{(0)} (p^2/k^2) - 2 \Lambda(k)$ . By construction,  $R^{(0)} (p^2/k^2) \approx 1$  for  $p^2 \ll k^2$ ; hence the propagator for low-eigenvalue graviton modes is

$$\left[ p^2 + k^2 - 2 \Lambda(k) \right]^{-1}. \quad (14)$$

It contains a mass term  $+k^2$  which, as it should be, suppresses those modes in the infrared. The  $\beta$ -functions for  $g$  and  $\lambda$  are given by traces involving the propagator (14).<sup>4</sup> The crucial point is that the (euclidean!) propagator (14) can have a pole when  $\Lambda(k)$  is too large and positive. It occurs for  $\Lambda(k) \geq k^2/2$ , or equivalently  $\lambda(k) \geq 1/2$ , at  $p^2 = 2 \Lambda(k) - k^2$ . Upon performing the  $p^2$ -sum this pole is responsible for the terms  $\propto 1/(1 - 2\lambda)$  and  $\ln(1 - 2\lambda)$  in the  $\beta$ -functions which become singular at  $\lambda = 1/2$ . The allowed part of the  $g$ - $\lambda$ -plane ( $\lambda < 1/2$ ) shown in Fig. 1 corresponds to the situation  $k^2 > 2 \Lambda(k)$  where the singularity is avoided thanks to the large regulator mass. As for the behavior of the RG trajectories near the boundary the crucial question is whether, when  $k$  is lowered,  $\Lambda(k)$  decreases at least as fast as  $k^2$  or slower. In the first case the trajectory would never reach the singularity, while it does so in the second. The trajectories of Type IIIa indeed belong

---

<sup>4</sup>To capture the essence of the argument it is sufficient to use a mass-type cutoff [12] for which  $R^{(0)} (p^2/k^2) \equiv 1$  for all  $p^2$ .

to the second case; since  $\Lambda(k)$  does not decrease fast enough the RG trajectory runs into the pole at a certain  $k_{\text{term}}$  where  $k_{\text{term}}^2 = 2\Lambda(k_{\text{term}})$ .

This phenomenon is well known from the investigation of spontaneous symmetry breaking in scalar field theory [12]. When one computes the running of the effective average potential  $U_k(\phi)$  in a polynomial truncation (expanding about  $\phi = 0$ ) the relevant propagator is of the form  $[p^2 + k^2 + m(k)^2]^{-1}$  where  $m(k)$  is the running mass. There is a pole at  $p^2 = -m(k)^2 - k^2$  if  $m(k)^2$  is negative and  $|m(k)^2| > k^2$ ; there is none in the symmetric phase ( $m(k)^2 > 0$ ). In fact, in the broken phase one finds terminating trajectories since  $-m(k)^2$  decreases too slowly when  $k$  is lowered. The cure to this problem is known [12]: If one uses a more general truncation, allowing for a non-polynomial  $U_k(\phi)$ , the RG trajectories never reach the singularity and extend to  $k = 0$ . Lowering  $k$ ,  $-m(k)^2$  decreases proportional to  $k^2$  in the broken phase and  $U_k(\phi)$  becomes convex with a flat bottom for  $k \rightarrow 0$  [12].

In this analogy  $m^2 > 0$  ( $m^2 < 0$ ) amounts to  $\Lambda < 0$  ( $\Lambda > 0$ ). The Type Ia (Type IIIa) trajectories correspond to the analog of the symmetric (broken) phase in the scalar theory. In a certain sense the Einstein–Hilbert truncation has a similar status as a polynomial truncation for  $U_k(\phi)$ : it is not general enough to be reliable down to  $k = 0$  for a positive cosmological constant or in the broken phase, respectively. While there are computationally manageable truncations of sufficient generality in the scalar case (local potential approximation with arbitrary  $U_k$ ), it is not known which truncations would allow for a reliable continuation of the Type IIIa trajectories below  $k_{\text{term}}$ . They are likely to contain nonlocal invariants [8, 16, 38] which are hard to handle analytically.

In view of the above analogy it is a plausible and very intriguing speculation that, for  $k \rightarrow 0$ , an improved truncation has a similar impact on the RG flow as it has in the scalar case. There the most important renormalization effect is the running of the mass:  $-m(k)^2 \propto k^2$ . If gravity avoids the singularity in an analogous fashion the cosmological constant would run proportional to  $k^2$ ,

$$\Lambda(k) = \lambda_*^{\text{IR}} k^2 \tag{15}$$

with a constant  $\lambda_*^{\text{IR}} < 1/2$ . In dimensionless units (15) reads  $\lambda(k) = \lambda_*^{\text{IR}}$ , i.e.  $\lambda_*^{\text{IR}}$  is a fixed point of the  $\lambda$ -evolution. If the behavior (15) is actually realized, the renormalized cosmological constant observed at very large distances,  $\Lambda(k \rightarrow 0)$ , vanishes regardless of

its bare value. Clearly this would have an important impact on the cosmological constant problem [39].

### 3 The RG trajectory realized in Nature: the Einstein–Hilbert domain

How can we find out which one of the RG trajectories shown in Fig. 1 is realized in Nature? As in every quantum field theory, one has to experimentally determine the value of appropriate “renormalized” quantities.<sup>5</sup> In Quantum Electrodynamics (QED), for instance, one measures the electron’s charge and mass in a large–distance experiment, thus fixing  $e(k)$  and  $m_e(k)$  at  $k = 0$ . In QCD the point  $k = 0$  is inaccessible, both theoretically and experimentally, so one uses a “renormalization point” at a higher scale  $k > 0$ . In QEG the situation is similar. In the extreme infrared ( $k \rightarrow 0$ ) we have neither theoretically reliable predictions nor precise experimental determinations of the gravitational couplings  $g$  and  $\lambda$ .

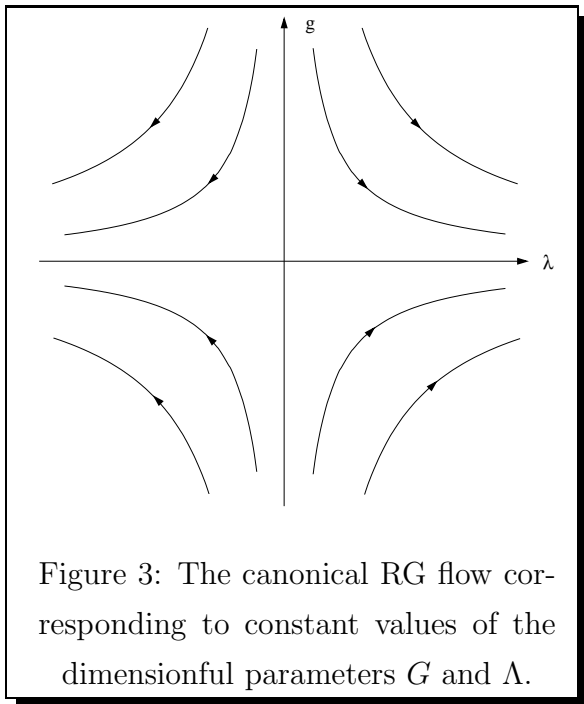
#### 3.1 Exploiting experimental information

We know that all gravitational phenomena at distance scales ranging from terrestrial experiments to solar system measurements are well described by standard General Relativity (GR). Since this theory is based upon the Einstein–Hilbert action with constant values of  $G$  and  $\Lambda$ , we can conclude that the RG evolution of those parameters for  $k$  between the related typical mass scales  $(1 \text{ meter})^{-1}$  and  $(1 \text{ astronomical unit})^{-1}$ , say, is negligibly small. In this “GR regime” the renormalization group flow is essentially the canonical one, i. e.  $g(k) \propto k^2$  and  $\lambda(k) \propto 1/k^2$  which follows from  $g(k) \equiv k^2 G(k)$ ,  $\lambda(k) \equiv \Lambda(k)/k^2$  when  $G, \Lambda = \text{const}$ . The corresponding RG trajectories are the hyperbolas  $g \propto 1/\lambda$  depicted in Fig. 3. During the  $k$ –interval defining the GR regime the true

---

<sup>5</sup>Above we considered pure gravity, while the experimental data include renormalization effects due to matter fields. Since in this paper we are interested in order of magnitude estimates only, and we anyhow do not know the exact matter field content of Nature, we assume that the inclusion of matter does not change the general qualitative features of pure gravity. As for the nonperturbative renormalizability it is known that there exist matter systems with this property and that they are “generic” in a sense [7].

RG trajectory realized in Nature must be very close to one of those hyperbolas.

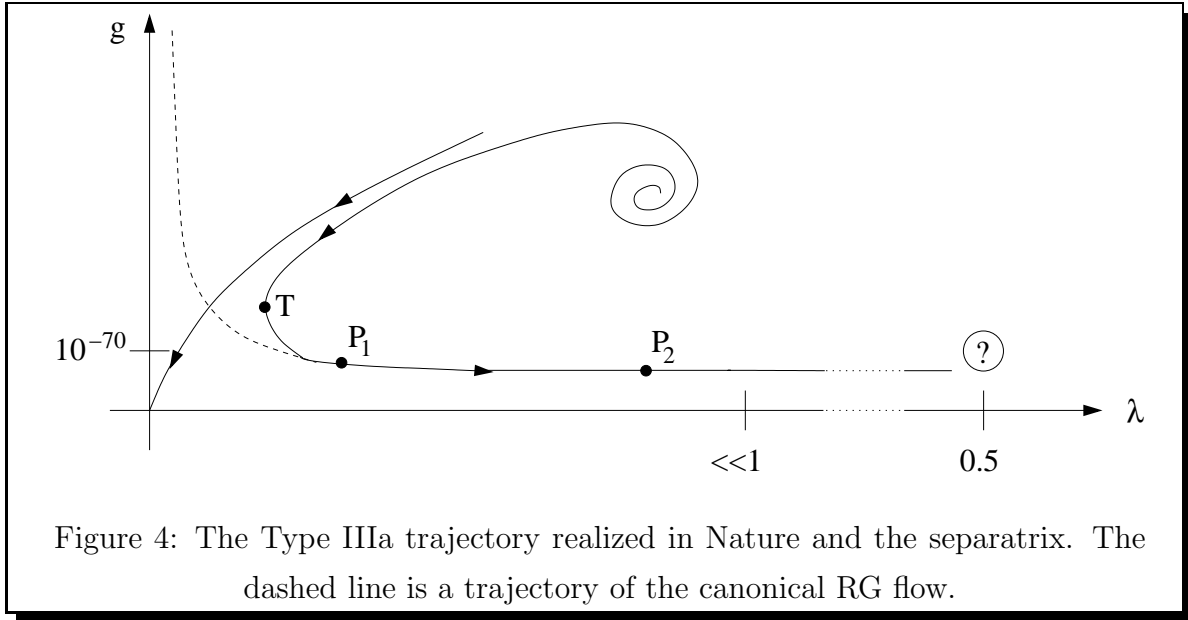


Which class does this trajectory belong to? Recent CMBR and high redshift supernova data show that the present Universe is in a state of accelerated expansion which, in a Friedmann–Robertson–Walker framework, can be explained by a nonzero *positive* cosmological constant. In the RG context this should mean that  $\Lambda(k \approx H_0) > 0$  since the relevant scale is set by  $H_0$ , the present Hubble parameter. Among the trajectories of the Einstein–Hilbert truncation only those of Type IIIa and IIIb run towards positive  $\Lambda$ 's for  $k \searrow 0$ .

Trajectories of Type IIIb correspond to a negative  $G$  and are excluded therefore. Thus *the RG trajectory realized in Nature, as long as it remains in the domain of validity of the Einstein–Hilbert truncation, belongs to Type IIIa.*

We saw that trajectories of Type IIIa cannot be continued below a certain  $k_{\text{term}}$ , and in the present paper we are going to argue that  $k_{\text{term}}$  is roughly of the order of typical galaxy scales. As a result, the Einstein–Hilbert truncation is probably insufficient to describe the (continuation of the) Type IIIa trajectory realized in Nature at the cosmological scale  $k \approx H_0$  where  $\Lambda$  was actually measured. Nevertheless it seems to be clear that, for  $k$  large enough, the true RG trajectory selected by Nature is a Einstein–Hilbert trajectory of Type IIIa. The reason is that the other alternatives, Type Ia and Type IIa, can be computed reliably down to  $k = 0$ , and they do *not* give rise to a positive cosmological constant in the infrared.

For our picture to be correct, the prospective Type IIIa trajectory must contain a sufficiently long “GR regime” where it runs on top of one of the hyperbolas of Fig. 3. The situation is sketched qualitatively in Fig. 4. The Type IIIa trajectory spirals out of the NGFP, approaches the separatrix, runs almost parallel to it for a while, then “turns left”



near the GFP, and finally runs towards the singularity at  $\lambda = 1/2$ . After the turning point where  $\partial_t \lambda = 0$ , but before it gets too close to  $\lambda = 1/2$ , this trajectory is an almost perfect hyperbola of the canonical RG flow. In Fig. 4 we indicate the latter by the dashed line which, between the points  $P_1$  and  $P_2$ , is indistinguishable from the Type IIIa trajectory. It is this segment between  $P_1$  and  $P_2$  which can be identified with the realm of classical GR. As we shall see in a moment, the variation of  $G$  and  $\Lambda$  along the true Type IIIa trajectory is unmeasurably small between  $P_1$  and  $P_2$ .

Which one of the infinitely many Type IIIa trajectories did Nature pick? We can answer this question if, from experiments or astrophysical observations, we know a single point  $(g, \lambda)$  the trajectory passes through. Let us assume we measure the (dimensionful) Newton constant and cosmological constant in a “laboratory” with a typical linear dimension of the order  $1/k_{\text{lab}}$ . We interpret the result of the measurements as the running couplings evaluated at this scale:  $G(k_{\text{lab}})$ ,  $\Lambda(k_{\text{lab}})$ . Knowing those two values, as well as the pertinent “laboratory” scale  $k_{\text{lab}}$ , we can compute the dimensionless couplings:

$$g(k_{\text{lab}}) = k_{\text{lab}}^2 G(k_{\text{lab}}), \quad \lambda(k_{\text{lab}}) = \Lambda(k_{\text{lab}})/k_{\text{lab}}^2. \quad (16)$$

The pair  $(g(k_{\text{lab}}), \lambda(k_{\text{lab}}))$  uniquely fixes a trajectory in the Einstein–Hilbert approximation. If one uses a more general truncation, further parameters need to be measured, of

course. The first one of the eqs. (16) can be rewritten in the following suggestive form:

$$g(k_{\text{lab}}) = (k_{\text{lab}}/m_{\text{Pl}})^2 \equiv (\ell_{\text{Pl}}/k_{\text{lab}}^{-1})^2. \quad (17)$$

Here we defined the Planck length and mass in the usual way in terms of the measured Newton constant  $G(k_{\text{lab}})$  according to  $\ell_{\text{Pl}} \equiv m_{\text{Pl}}^{-1} = \sqrt{G(k_{\text{lab}})}$ .

Newton's constant has been measured at length scales  $k_{\text{lab}}^{-1}$  ranging from the size of terrestrial experiments to solar system dimensions. Within the errors the result has always been the same:  $G(k_{\text{lab}}) = G_{\text{lab}} \equiv 6.67 \cdot 10^{-11} \text{ m}^3 \text{ kg}^{-1} \text{ s}^{-2}$ . We can now calculate  $g(k_{\text{lab}})$  according to (16). At the typical scale of a terrestrial laboratory one finds

$$g(k_{\text{lab}}) \approx 10^{-70} \quad \text{for } k_{\text{lab}}^{-1} = 1 \text{ m} \quad (18)$$

while at the solar system scale of 1 astronomical unit,

$$g(k_{\text{lab}}) \approx 10^{-92} \quad \text{for } k_{\text{lab}}^{-1} = 1 \text{ AU}. \quad (19)$$

In any case  $g(k_{\text{lab}})$  is an extremely small number for any  $k_{\text{lab}}$  in the GR regime,  $g(k_{\text{lab}}) \lll 1$ . Its precise value will not matter in the following; for the sake of clarity we shall use the example  $k_{\text{lab}}^{-1} = 1$  meter and  $g(k_{\text{lab}}) \approx 10^{-70}$  for numerical illustration. Throughout the discussion the length scale  $k_{\text{lab}}^{-1}$  is assumed to lie in the GR regime, ranging from terrestrial to solar system distances.

The determination of the associated  $\lambda(k_{\text{lab}})$  is difficult; in fact, rather than at ‘‘laboratory’’ scales  $1 \text{ m} \cdots 1 \text{ AU}$ ,  $\Lambda$  was actually measured at cosmological distance scales. For a first qualitative discussion the following estimate is sufficient, however. According to the effective vacuum Einstein equation at the scale  $k_{\text{lab}}$ , a cosmological constant of magnitude  $\Lambda(k_{\text{lab}})$  leads to the spacetime whose radius of curvature is of the order

$$r_c \approx \Lambda(k_{\text{lab}})^{-1/2} = \lambda(k_{\text{lab}})^{-1/2} k_{\text{lab}}^{-1}.$$

We know that in absence of matter, at  $k_{\text{lab}}^{-1} = 1 \text{ m}$ , say, spacetime (when observed with a ‘‘microscope’’ of resolution  $k_{\text{lab}}^{-1}$ ) is flat with a very high precision, i. e. that  $r_c$  is much larger than the size of the ‘‘laboratory’’:  $r_c \gg k_{\text{lab}}^{-1}$ . As a consequence,  $\lambda(k_{\text{lab}})$  must be very small compared to unity:

$$\lambda(k_{\text{lab}}) \lll 1. \quad (20)$$

This means in particular that, at  $k_{\text{lab}}$  and in the entire GR regime, the trajectory realized in Nature is still very far away from the dangerous singularity at  $\lambda = 1/2$  where the Einstein–Hilbert approximation breaks down.

### 3.2 Approximate RG flow near the GFP

Since  $g, \lambda \ll 1$  in the GR regime we may neglect higher order terms  $g^2, g\lambda, \dots$  in the eqs. (10) and obtain the following flow equation linearized about the GFP:

$$\partial_t \lambda = -2 \lambda + \varphi_2 g / \pi \tag{21a}$$

$$\partial_t g = 2 g. \tag{21b}$$

In the “linear regime” where (21) is valid, only the cosmological constant shows a non-canonical running, while the dimensionful Newton constant does not evolve in the approximation (21b).

In the next to leading order  $G$  runs according to  $\partial_t G = \eta_N G$  with  $\eta_N = -b g$  proportional to  $g$ . In any cutoff scheme  $b$  is a positive constant of order unity,  $b = (24 - \varphi_1) / 3\pi$  for the sharp cutoff. Hence

$$-\eta_N \Big|_{\text{RG regime}} \approx 10^{-70} \dots 10^{-92}. \tag{22}$$

The smallness of these numbers explains the success of standard General Relativity based upon the approximation  $\eta_N = 0$ , and it confirms our interpretation of the segment between the points  $P_1$  and  $P_2$  in Fig. 4 as the realm of classical gravity.

To the right of the point  $P_2$  in Fig. 4, at scales  $k$  lower than those of the GR regime, the growth of  $G(k)$  due to the infrared instability sets in.

Let us return to the linearized flow equations (21). They are applicable whenever the trajectory is close to the GFP ( $g, \lambda \ll 1$ ), not only in the GR regime. We may use them to derive a relation between the coordinates  $(g_T, \lambda_T)$  of the trajectory’s turning point  $T$  at which it switches from decreasing to increasing values of  $\lambda$ . (See Fig. 4.) Setting  $\partial_t \lambda = 0$  in (21a) we obtain

$$\lambda_T = (\varphi_2 / 2\pi) g_T. \tag{23}$$

The constant  $\varphi_2$  is cutoff scheme-, i. e.  $R^{(0)}$ -dependent, but it is of order unity for any cutoff. Therefore

$$\lambda_T/g_T = \mathcal{O}(1). \quad (24)$$

Eqs. (23), (24) are valid provided  $g_T, \lambda_T \ll 1$ . Later on we shall see that this is actually the case in Nature.

After the trajectory has passed the turning point,  $g$  keeps decreasing and  $\lambda$  increases. As a result, the second term on the RHS of (21a),  $\varphi_2 g/\pi$ , gradually becomes negligible compared to the first one,  $-2\lambda$ , so that the flow equation becomes the canonical one. This marks the beginning of the GR regime at  $P_1$ .

It is easy to solve the coupled differential equations (21) exactly. They allow for two free constants of integration which we fix by requiring  $g(k_T) = g_T$  and  $\lambda(k_T) = \lambda_T$ . By definition,  $k_T$  is the scale at which the trajectory passes through the turning point. The solution reads

$$g(k) = g_T \left( \frac{k}{k_T} \right)^2 \quad (25a)$$

$$\lambda(k) = \frac{1}{2} \lambda_T \left( \frac{k_T}{k} \right)^2 \left[ 1 + \left( \frac{k}{k_T} \right)^4 \right]. \quad (25b)$$

The corresponding running of the dimensionful parameters is given by

$$G(k) = \frac{g_T}{k_T^2} = \text{const} \quad (26a)$$

$$\Lambda(k) = \frac{1}{2} \lambda_T k_T^2 \left[ 1 + \left( \frac{k}{k_T} \right)^4 \right]. \quad (26b)$$

Since the linear regime contains the GR regime, we may identify the constant in (26a) with  $G_{\text{lab}} \equiv m_{\text{Pl}}^{-2}$ . This entails the important relation  $k_T^2 = g_T m_{\text{Pl}}^2$ , or

$$k_T = \sqrt{g_T} m_{\text{Pl}}. \quad (27)$$

We observe that a small  $g_T \ll 1$  will lead to a large hierarchy  $m_{\text{Pl}} \gg k_T$ .

We can use (27) in order to eliminate  $k_T$  from (25):

$$g(k) = \left( \frac{k}{m_{\text{Pl}}} \right)^2 \quad (28a)$$

$$\lambda(k) = \frac{1}{2} g_T \lambda_T \left( \frac{m_{\text{Pl}}}{k} \right)^2 \left[ 1 + \frac{k^4}{g_T^2 m_{\text{Pl}}^4} \right]. \quad (28b)$$

For later use we note that for any  $k$  in the linear regime

$$G(k) \Lambda(k) = g(k) \lambda(k) = \frac{1}{2} g_T \lambda_T \left[ 1 + \left( \frac{k}{k_T} \right)^4 \right]. \quad (29)$$

Looking at eqs. (26a,b) we see that, while  $G$  does not run at all in the linear regime, the scale dependence of  $\Lambda$  is entirely due to the factor  $[1 + (k/k_T)^4]$ . Once  $k$  has become much smaller than  $k_T$ , after the trajectory has “turned left”, this factor approaches unity, and  $\Lambda$  effectively stops to run. By definition, this happens at  $P_1$ , the starting point of the GR regime.

Let us make this statement more precise. Denoting by  $k_1$  the scale at which the trajectory passes through  $P_1$ , the requirement is that  $(k_1/k_T)^4 \ll 1$ . We quantify the precision with which the  $k^4$ -term is negligible in the GR regime by means of an exponent  $\nu$ . In terms of  $\nu$ , we define  $k_1$  by

$$k_1/k_T = 10^{-\nu}. \quad (30)$$

As a result,  $(k/k_T)^4$  is smaller than  $10^{-4\nu}$  for all scales in the GR regime ( $k < k_1$ ). A value such as  $\nu = 1$  should be sufficient in practice. It makes sure that in the GR regime  $\Lambda$  is constant with a precision better than 0.01 %.

For  $k$  any scale in the GR regime we obtain from (28), in very good approximation,

$$g(k) = (k/m_{\text{Pl}})^2 \quad (31a)$$

$$\lambda(k) = \frac{1}{2} g_T \lambda_T (m_{\text{Pl}}/k)^2. \quad (31b)$$

Similarly (26) yields the following constant values of the dimensionful quantities:

$$G(k) = G_{\text{lab}} \quad (32a)$$

$$\Lambda(k) = \frac{1}{2} \lambda_T k_T^2 = \frac{1}{2} \Lambda(k_T). \quad (32b)$$

Remarkably, in the GR regime,  $\Lambda$  differs from its value at the turning point precisely by a factor of 1/2. As a trivial consequence,

$$(G\Lambda) \Big|_{\text{GR regime}} = \frac{1}{2} (G\Lambda) \Big|_{\text{turning point}} \quad (33a)$$

and (29) reduces to

$$G(k) \Lambda(k) = g(k) \lambda(k) = \frac{1}{2} g_T \lambda_T \quad (33b)$$

We shall come back to this relationship later on.

Next we derive various estimates for  $g$  and  $\lambda$  at  $k_T$  and  $k_1$ . If we evaluate (25) at  $k = k_1$ , neglecting the  $k^4$ -term in (25b), and use (30) we find<sup>6</sup>

$$g(k_1) = g_T 10^{-2\nu} \quad (34a)$$

$$\lambda(k_1) = \lambda_T 10^{+2\nu}. \quad (34b)$$

Obviously  $P_1$  has a  $g$ - ( $\lambda$ -) coordinate which is smaller (larger) than the corresponding coordinate of  $T$  by a factor  $10^{-2\nu}$  ( $10^{+2\nu}$ ), as it should be according to Fig. 4. Now we exploit eq. (24). Neglecting factors of order 1 we have  $g_T = \lambda_T$  which yields when combined with (34)

$$g(k_1) = \lambda(k_1) 10^{-4\nu}. \quad (35)$$

Since  $\lambda$  increases along the trajectory we know that  $\lambda_T < \lambda(k_1) < \lambda(k_{\text{lab}})$  where  $k_{\text{lab}}$  is any “laboratory” scale in the GR regime. Therefore, as a consequence of the experimental result (20),

$$\lambda_T < \lambda(k_1) < \lambda(k_{\text{lab}}) \ll 1. \quad (36)$$

Since  $\lambda_T$  and  $g_T$  are almost equal,  $g_T$  is small, too:

$$g_T \approx \lambda_T \ll 1. \quad (37)$$

According to (35),  $g(k_1)$  is even smaller than  $\lambda(k_1)$ . Hence, with  $\lambda(k_1) \ll 1$  from (36), it follows that

$$g(k_1) \ll 1, \quad \lambda(k_1) \ll 1. \quad (38)$$

Eqs. (37) and (38) show that for the RG trajectory realized in Nature the points  $T$  and  $P_1$  are located at an extremely short distance to the GFP. The trajectory starts at

---

<sup>6</sup>In order-of-magnitude equations such as (34) we suppress inessential factors of order unity.

the NGFP with coordinates  $g_*, \lambda_* = \mathcal{O}(0.1)$  [3, 5]. Then it follows the separatrix until, at very tiny values of  $g$  and  $\lambda$ , it gets ultimately driven away from the GFP along its unstable  $\lambda$ -direction. In pictorial terms we can say that the trajectory is squeezed deeply into the wedge formed by the separatrix and the  $g = 0$ -axis. As a consequence, it spends a very long RG time near the GFP because the  $\beta$ -functions are small there. In this sense the RG trajectory which Nature has selected is highly non-generic or “unnatural”. It requires a precise fine-tuning of the initial conditions, to be posed infinitesimally close to the NGFP.

### 3.3 Existence of a GR regime and the cosmological constant problem

Why did Nature pick a trajectory which gets so “unnaturally” close to the GFP? Why not, for example, one of those plotted in Fig. 1 which always keep a distance of order unity to the GFP and require no special fine-tuning? Of course questions of this kind cannot be answered within QEG, for the same reason one cannot compute the electron’s charge or mass in QED.

However, it is fairly easy to show that a Universe based upon one of the generic trajectories would look very different from the one we know. The main difference is that, along a generic trajectory, no sufficiently long GR regime would exist where classical gravity makes sense at all. According to our previous discussion, the GR regime is located in between a regime with strong UV renormalization effects (spiraling around the NGFP related to asymptotic safety) and, most probably, a second regime with a significant running of the parameters in the IR. For classical GR to be applicable the UV and IR regimes must be well separated. For a generic trajectory this is not the case, however. The generic Einstein–Hilbert trajectories computed in [8] leave the UV regime at  $k \approx m_{\text{Pl}}$  and soon after they terminate at a  $k_{\text{term}}$  not much smaller than  $m_{\text{Pl}}$ ; there is no GR regime which would last for a few orders of magnitude at least.

The basic mechanism which allows for the emergence of a GR regime is to fine-tune the trajectory in such a way that it spends a lot of RG time near the GFP. In this manner the onset of the IR regime, within the Einstein–Hilbert truncation characterized by the value of  $k_{\text{term}}$ , gets enormously delayed,  $k_{\text{term}}$  being much smaller than  $m_{\text{Pl}}$ . If classical

GR is correct up to a length scale  $L$ , the trajectory must be such that its  $k_{\text{term}}^{-1}$  is larger than  $L$  since at  $k_{\text{term}}^{-1}$  the IR effects are likely to become visible.

A quantitative estimate of  $k_{\text{term}}$  can be obtained as follows. In the linear regime the RG flow is explicitly given by eqs. (25). Once  $k$  is sufficiently low we leave this regime and the full nonlinear Einstein–Hilbert flow equations have to be used. At even smaller scales, the truncation breaks down and we should switch to a more general one. Outside the linear regime, the  $\beta$ -functions are no longer small, hence the trajectory has a comparatively high “speed” there. As a result, it takes the trajectory much longer to go from  $T$  to the boundary of the linear, i. e. GR regime than from there to a point close to  $\lambda = 1/2$ . Therefore we may use eq. (31b) for  $\lambda(k)$  in the GR regime in order to derive an estimate for  $k_{\text{term}}$ . We identify  $k_{\text{term}}$  with the scale where, according to (31b), the value  $\lambda = 1/2$  is reached:  $g_T \lambda_T (m_{\text{Pl}}/k_{\text{term}})^2 = 1$ . In this rough approximation,

$$k_{\text{term}} = \sqrt{g_T \lambda_T} m_{\text{Pl}} \quad (39a)$$

$$= (\varphi_2/2\pi)^{1/2} g_T m_{\text{Pl}} \quad (39b)$$

or, in terms of length scales,

$$k_{\text{term}}^{-1} = \frac{\ell_{\text{Pl}}}{\sqrt{g_T \lambda_T}}. \quad (40)$$

This equation shows explicitly that by making  $g_T \approx \lambda_T$  small,  $k_{\text{term}}^{-1}$  can be made as large as we like.

Thus we have demonstrated that *only a “non-generic” trajectory with an “unnaturally” small  $g_T \approx \lambda_T \ll 1$  does give rise to a long GR regime comprising many orders of magnitude.*

In (27) we saw that the turning point is passed at  $k_T = \sqrt{g_T} m_{\text{Pl}}$ . Ignoring the  $\mathcal{O}(1)$ -factor  $(\varphi_2/2\pi)$  in (39b) this entails  $k_{\text{term}} = \sqrt{g_T} k_T$ . As a result, there exists an exactly symmetric “double hierarchy” among the three mass scales  $k_{\text{term}}$ ,  $k_T$ , and  $m_{\text{Pl}}$ :

$$\frac{k_{\text{term}}}{k_T} = \sqrt{g_T} \ll 1, \quad \frac{k_T}{m_{\text{Pl}}} = \sqrt{g_T} \ll 1. \quad (41)$$

Therefore, on a logarithmic scale,  $k_T$  is precisely in the middle between  $m_{\text{Pl}}$  and  $k_{\text{term}}$ . Thanks to the smallness of  $g_T$  it is many orders of magnitude away from either end.

The emergence of a long regime where gravity is essentially classical is one of the benefits we get from the unnaturalness of the trajectory chosen by Nature. Another one is

that, in this classical regime, the cosmological constant is automatically small. Inserting (27) into (32b) we obtain the following  $\Lambda$  in the GR regime:

$$\Lambda(k) = \frac{1}{2} g_T \lambda_T m_{\text{Pl}}^2 = \text{const.} \quad (42)$$

Again thanks to the smallness of  $g_T$  and  $\lambda_T$ , the cosmological constant is much smaller than  $m_{\text{Pl}}^2$ . Up to a factor of order unity,

$$\left. \frac{\Lambda}{m_{\text{Pl}}^2} \right|_{\text{GR regime}} = g_T^2 \ll 1. \quad (43)$$

Thus we may conclude that the very fine-tuning which gives rise to a long GR regime at the same time implies a large hierarchy between the  $\Lambda$  in this GR regime and  $m_{\text{Pl}}^2$ , which often is considered its “natural” value.

This observation provides a solution to the “cosmological constant problem” by realizing that it is actually part of a much more general naturalness problem. Rather than “Why is  $\Lambda$  so small?” the new question is “Why does gravity behave classically over such a long interval of scales?”.

The basic reason for this connection is very simple. Denoting the cosmological constant in the GR regime by  $\Lambda(k_{\text{lab}}) \equiv \Lambda_{\text{lab}}$  we have  $\lambda(k) = \Lambda_{\text{lab}}/k^2$  there. This  $\lambda(k)$  approaches unity so that the IR renormalization effects become strong once  $k$  is of the order  $\sqrt{\Lambda_{\text{lab}}}$ . Hence, roughly,

$$k_{\text{term}} \approx \sqrt{\Lambda_{\text{lab}}} \quad (44)$$

which shows that  $k_{\text{term}}$  is small if, and only if,  $\Lambda_{\text{lab}}$  is small.

This is precisely what one finds by numerically solving the flow equations: There do not exist any Type IIIa trajectories which, on the one hand, admit a long classical regime, and on the other hand, have a large cosmological constant. As a consequence, *the smallness of the cosmological constant poses no naturalness problem beyond the one related to the very existence of a classical regime in the Universe.*

Strictly speaking this resolution of the cosmological constant problem is only a partial one for the following reasons. (1) We analyzed the flow equations of pure gravity only, but we believe that the inclusion of matter fields (forming symmetry breaking condensates, etc.) will not change the general picture. Since anyhow only massless particles

contribute to the  $\beta$ -functions for  $k \rightarrow 0$ , it is hardly possible that the matter fields destroy the IR renormalizations near  $\lambda = 1/2$ . But if they survive the estimate (44) remains intact, again implying that a long GR regime requires a small  $\Lambda_{\text{lab}}$ . (2) Our argument refers to  $\Lambda_{\text{lab}}$  rather than the cosmologically relevant  $\Lambda(H_0)$ . Because of the IR effects,  $\Lambda_{\text{lab}}$  and  $\Lambda(H_0)$  differ in principle, but we shall see later on that in Nature this difference is small compared to the notorious 120 orders of magnitude one has to cope with.

In fact, the upper boundary of the linear regime is roughly the Planck scale since, according to (28),  $g(k)$  and  $\lambda(k)$  are of the order of  $g_*$  and  $\lambda_*$  slightly below  $k = m_{\text{Pl}}$ . Between this scale and the turning point the change of  $\Lambda$  is enormous. From (26b) with (27) and (37) we obtain  $\Lambda(m_{\text{Pl}}) = \frac{1}{2} \Lambda(k_T)/g_T^2 \gg \Lambda(k_T)$ . In the next section we shall see that  $g_T \approx 10^{-60}$ , whence  $\Lambda(k_T) \approx 10^{-120} \Lambda(m_{\text{Pl}})$ .

### 3.4 Is the Hubble scale within the classical regime?

The observational (CMBR, supernova, etc.) data, when interpreted within standard cosmology, show that the present vacuum energy density of the Universe is very close to the critical one, implying that  $\Lambda$  is of the order of  $H_0^2$ . (The general relationship is  $\Lambda = 3\Omega_\Lambda H_0^2$ , and the data favor  $\Omega_\Lambda \approx 0.7$ ).

We can now ask whether, if  $\Lambda$  is as large as  $H_0^2$ , the Hubble scale is still within the GR regime. If we interpret  $H_0^2$  as a ‘‘laboratory’’ value,  $\Lambda_{\text{lab}} \approx H_0^2$ , the estimate (44) yields

$$k_{\text{term}} \approx H_0. \tag{45}$$

This is a very remarkable and intriguing result: *On the RG trajectory Nature has picked, the Hubble scale  $k = H_0$  is precisely at the boundary of the GR regime.* At distances small compared to the Hubble length  $\ell_H \equiv H_0^{-1}$  classical GR is a good approximation, but on length scales  $\ell \gtrsim \ell_H$  the IR renormalization effects become important so that its use is questionable there.

Since  $k = H_0$  is just at the boundary of the GR regime it is plausible to assume that the cosmological values  $G(H_0)$  and  $\Lambda(H_0)$  do not differ too much from  $G_{\text{lab}}$  and  $\Lambda_{\text{lab}}$ , respectively. (Later on we shall see that the difference should not be more than one or two orders of magnitude.) If so, we are in a position to completely fix the parameters

of the RG trajectory because we can fit the measured  $\Lambda$ -value to the trajectories of the linearized flow. Inserting  $k = H_0$ ,  $\Lambda(k) = H_0^2$ , and  $G(k) = m_{\text{Pl}}^{-2}$  into (33b) we find

$$\frac{1}{2} g_T \lambda_T = g(k) \lambda(k) = (H_0/m_{\text{Pl}})^2. \quad (46)$$

Since  $g_T$  and  $\lambda_T$  are approximately equal, and since the “experimental” value for  $H_0/m_{\text{Pl}}$  is known to be about  $10^{-60}$ , eq. (44) allows for an explicit determination of  $g_T$  and  $\lambda_T$ :

$$g_T \approx \lambda_T \approx H_0/m_{\text{Pl}} \approx 10^{-60}. \quad (47)$$

This number is indeed extremely small but, consistently with the picture drawn so far, still larger than  $g(k_{\text{lab}}) \lesssim 10^{-70}$ .

With (47) the “double hierarchy” (41) comprises 30 orders of magnitude between  $k_{\text{term}}$  and  $k_T$ , and between  $k_T$  and  $m_{\text{Pl}}$ , respectively. Combining eq. (39a) for  $k_{\text{term}}$  with (46) we rediscover that  $k_{\text{term}} \approx H_0$ , and using eq. (27) we obtain the scale at the turning point:

$$k_T \approx \sqrt{H_0 m_{\text{Pl}}} \approx 10^{-30} m_{\text{Pl}}. \quad (48)$$

The associated length scale is

$$k_T^{-1} \approx 10^{30} \ell_{\text{Pl}} \approx 10^{-3} \text{ cm}. \quad (49)$$

It is very exciting that this is a truly macroscopic length scale, very far away from the Planck regime which is usually thought to be the realm of the quantum gravitational UV renormalization effects. Note that the “turning left” of the trajectory, despite the large value of (49), is still an effect of the “UV type” in the sense that it has nothing to do with the IR phenomena occurring when  $\lambda \approx 1/2$ . It happens so extremely late because of the enormous fine-tuning of the trajectory.

Allowing a margin of one order of magnitude ( $\nu = 1$ ), say, (49) implies a beginning of the GR regime at

$$k_1^{-1} \approx 10^{-2} \text{ cm}. \quad (50)$$

At length scales  $\ell \equiv k^{-1}$  larger than this value  $\Lambda$  is constant with high precision. But for  $\ell \ll k_1^{-1}$  it has a strong scale dependence  $\propto k^4$  given by eq. (26b). Since  $\lambda_T k_T^2/2 = \Lambda_{\text{lab}} \approx H_0^2$  we may rewrite this equation in the form

$$\Lambda(k) \approx H_0^2 \left[ 1 + (k/k_T)^4 \right]. \quad (51)$$

Should we then expect to see strong violations of GR at the millimeter or micrometer scale? The answer is probably no. While the variation of  $\Lambda(k)$  is indeed very strong, between  $k^{-1} = 1 \mu\text{m}$  and  $k^{-1} = 1 \text{nm}$ , say, it changes by 12 orders of magnitude, the absolute value of  $\Lambda$  is proportional to  $H_0^2$  which is extremely tiny according to all standards of terrestrial experiments, of course. Because of the practical problems with measuring  $\Lambda$  at non-cosmological distances the running of  $\Lambda$  could possibly remain undetected over many orders of magnitude.

By combining (31) with (46) we obtain  $g$  and  $\lambda$  at the Hubble scale:

$$g(H_0) \approx 10^{-120}, \quad \lambda(H_0) = \mathcal{O}(1). \quad (52)$$

This approximation neglects the IR effects close to  $H_0$ , but should be correct as far as the orders of magnitude are concerned.

## 4 The RG trajectory realized in Nature: the deep IR

### 4.1 Leaving the GR regime

Denoting the scales corresponding to the boundary points of the GR regime,  $P_1$  and  $P_2$ , by  $k_1$  and  $k_2$ , respectively, the general picture of the trajectory which Nature has chosen can be summarized as follows. For  $k = \infty$  it starts infinitesimally close to the NGFP, runs very close to the separatrix until, at  $k_T$ , it turns left in the very last moment before hitting the GFP, at  $g_T, \lambda_T \ll 1$ , then enters the GR regime at the scale  $k_1$  and leaves it at  $k_2$ . In the entire GR regime  $G$  and  $\Lambda$  are constant, and  $\lambda(k) \ll 1$ .

At scales  $k < k_2$  immediately below the GR regime there exists a regime where the renormalization effects become appreciable, but are still weak enough for the Einstein–Hilbert truncation to be reliable. The mechanism discussed in Section 2 causes  $G(k)$  to increase with decreasing  $k$ . The dimensionless cosmological constant  $\lambda$  is still much smaller than 1/2 there.

At even smaller scales,  $\lambda$  approaches 1/2, and the Einstein–Hilbert truncation becomes unreliable as it would yield an unbounded growth of  $G(k)$  and  $\eta_N \rightarrow -\infty$ ,  $dG/dk \rightarrow -\infty$  at a nonzero  $k_{\text{term}}$ .

It is our main hypothesis that exact QEG or a sufficiently general truncation “tames” this divergent behavior and leads to a bounded growth of  $G(k)$ , i. e. a finite  $\eta_N$ , along a

RG trajectory which passes smoothly through  $k_{\text{term}}$  and can be continued to  $k = 0$ . We believe that those IR renormalization effects lead to observable physical effects, and that the scale at which they occur is approximately given by the value of  $k_{\text{term}}$  obtained from the Einstein–Hilbert truncation.

The truncations needed for a reliable ab initio computation of the IR effects within QEG are much more complicated than those used so far. They contain many more couplings beyond  $g$  and  $\lambda$ . The resulting RG trajectory can be visualized as a curve in a high dimensional “theory space” containing the  $g$ - $\lambda$ -plane as a subspace. In general one has to distinguish the projection of the exact trajectory onto the  $g$ - $\lambda$ -plane and the trajectory implied by the Einstein–Hilbert truncation whose theory space consists of this plane only. As long as this truncation is reliable the two curves in the  $g$ - $\lambda$ -plane do not differ much, but the deviations become large when the trajectory runs out of the domain of validity of the truncation. For the RG trajectory realized in Nature this is the case near the question mark in Fig. 4, close to  $\lambda = 1/2$ .

Clearly it would be desirable to employ such improved truncations which allow for a continuation of the Type IIIa trajectories to  $k = 0$ , but because of the enormous mathematical complexity of the resulting flow equations this seems to be out of reach using the presently available computational techniques. The situation is similar to QCD where the analogous nonperturbative IR phenomena such as color confinement or chiral symmetry breaking are notoriously difficult to deal with analytically.

It is of crucial importance to find out at which scale the IR effects become strong. In principle  $k_{\text{term}}$  can be determined by measuring  $G(k_{\text{lab}})$  and  $\Lambda(k_{\text{lab}})$  in the “laboratory” and integrating the Einstein–Hilbert flow equations towards smaller  $k$  until one reaches  $\lambda = 1/2$  at  $k_{\text{term}}$ . However, in practice this does not work because it is very hard to measure  $\Lambda$  in a non–cosmological “laboratory”.

A first hint about the value of  $k_{\text{term}}$  comes from the argument in Subsection 3.4. Given the measured value of  $\Lambda$ ,  $k_{\text{term}}$  is of the order of the Hubble scale. We take this as a strong indication suggesting that at least in cosmology the IR effects are “at work” already. However, in order to assess their relevance at galactic scales, a more precise estimate is needed.

Since we have no analytical tools yet to investigate those IR effects we can resort to the following phenomenological strategy for obtaining information about the RG tra-

jectory: We make an ansatz for the trajectory, work out its consequences, and compare them to the observational data. The so-called IR fixed point model developed in [32, 33] is an attempt in precisely this direction. In the next subsection we describe its status in the context of the present discussion.

## 4.2 The IR fixed point model

The IR fixed point model [32, 33] is a cosmology based upon the hypothesis that, for  $k \rightarrow 0$ , the projected trajectory  $(g(k), \lambda(k))$  runs into a non-Gaussian IR fixed point  $(g_*^{\text{IR}}, \lambda_*^{\text{IR}})$ , different from the UV fixed point it emanates from. This assumption implies that in the deep IR the dimensionful parameters run as

$$G(k) = g_*^{\text{IR}}/k^2, \quad \Lambda(k) = \lambda_*^{\text{IR}} k^2. \quad (53)$$

The behavior of  $\Lambda(k)$  is the same as in (15) which was motivated by the analogy with the scalar theory, and  $G(k) \propto 1/k^2$  is a plausible ansatz for the growth of Newton’s constant. Since  $\beta_g = (2 + \eta_N) g$  holds true in general, but not necessarily with the  $\eta_N$  of (5), the anomalous dimension at the fixed point is  $\eta_N = -2$ .

Note that while the IR renormalization according to (53) has a strong effect on  $G(k)$  and  $\Lambda(k)$  separately, it leaves the product  $G(k) \Lambda(k)$  invariant:  $\Lambda(k)$  decreases at the same rate  $G(k)$  increases towards the IR.

In a homogeneous and isotropic Universe the relevant cutoff scale is  $k = \widehat{\xi}/t$  to leading order<sup>7</sup> [31, 32]. Here  $t$  is the cosmological time and  $\widehat{\xi}$  is a constant of order unity. This “cutoff identification” turns  $G(k)$  and  $\Lambda(k)$  into functions of time:  $G(t) \equiv G(k = \widehat{\xi}/t)$ , and similarly for  $\Lambda$ . Replacing the constants  $G$  and  $\Lambda$  in the classical Einstein equation with  $G(t)$  and  $\Lambda(t)$  one obtains a “RG improved” field equation whose Robertson–Walker–type solutions can be studied [31, 32]. For the  $k$ –dependence (53) one finds an accelerating Universe with a scale factor  $a(t) \propto t^{4/3}$ . The fixed point not only forces the Universe to enter an epoch of accelerated expansion for  $t \rightarrow \infty$ , it also explains without any fine-tuning of parameters why in the late Universe the matter energy density equals approximately the vacuum energy density, thus providing a natural solution to the “cosmic coincidence puzzle”. Confronting the infrared fixed point model with the

---

<sup>7</sup>We consider only power law solutions for which  $\widehat{\xi}/t$  is proportional to the Hubble parameter  $H(t)$ .

observational data (supernovae, compact radio sources, CMBR, etc.) it performs as well as the best-fit Friedmann model. (See ref. [33] for further details.)

The fixed point solution to the improved Einstein equation exists only if  $\lambda_*^{\text{IR}}$  and  $\widehat{\xi}$  are such that  $\lambda_*^{\text{IR}} \widehat{\xi}^2 = 8/3$ , implying that  $\lambda_*^{\text{IR}}$  has to be of order unity since  $\widehat{\xi} = \mathcal{O}(1)$ . Furthermore,  $g_*^{\text{IR}}$  is found to be of the order  $[G(t_0)/G_{\text{lab}}] (H_0/m_{\text{Pl}})^2$ . Here  $G(t_0)$  denotes the present Newton constant at cosmological scales. According to the analysis of ref. [33], the observational data imply that the ratio  $G(t_0)/G_{\text{lab}}$  can comprise at most one or two orders of magnitude (in any case a number by far smaller than 120, say). Therefore, using  $H_0/m_{\text{Pl}} \approx 10^{-60}$ , we find that the model is consistent only provided

$$g_*^{\text{IR}} \approx 10^{-120}, \quad \lambda_*^{\text{IR}} \approx \mathcal{O}(1). \quad (54)$$

This model is based upon the assumption that the IR effects lead to the formation of a fixed point into which the trajectory is attracted for  $k \rightarrow 0$ . The solubility of the improved Einstein equation and the observational data then require that the projection of the fixed point onto the  $g$ - $\lambda$ -plane is located at the coordinates (54). The comparison with (52) shows that the point  $(g_*^{\text{IR}}, \lambda_*^{\text{IR}})$  is precisely in the region where the Einstein-Hilbert approximation breaks down and something new must happen. (Near the question mark in Fig. 4.)

This consistency is an important success of the fixed point model. It describes the simplest possible behavior of the (projected) RG trajectory in the deep IR: the strong quantum corrections near  $\lambda = 1/2$  simply bring the running of  $g(k)$  and  $\lambda(k)$  to a complete standstill, at  $g_*^{\text{IR}}$  and  $\lambda_*^{\text{IR}}$ , respectively.

We can think of the cosmological time evolution as an evolution of the Universe along the RG trajectory with  $k$  corresponding to  $1/t$  or  $H(t)$ , which is essentially the same here. As long as the Universe stays in the GR regime the classical Friedmann equations are a valid description, but as soon as  $\lambda$  gets close to  $1/2$  the fixed point cosmology takes over, the Universe starts accelerating, and the vacuum and matter energy densities become approximately equal ( $\Omega_\Lambda \approx \Omega_M$ ). These predictions are in remarkable agreement with what we learned about the Universe from the astrophysical data which became available during the past few years. (See refs. [32, 33] for further details.)

Even if the finer details of the IR fixed point model are perhaps not completely correct quantitatively it demonstrates that an increase (decrease) of  $G$  ( $\Lambda$ ) near the Hub-

ble scale would explain many of the observed features of the late Universe in an extremely natural way. In a sense, the renormalization effects would mimic the presence of “quintessence” which was invented in order to explain these features.

### 4.3 Where does the IR running set in?

Motivated by the estimate  $k_{\text{term}} \approx H_0$  from Subsection 3.4 and the phenomenological success of the IR fixed point model we believe that at the present Hubble scale the IR effects have an observable and qualitatively important impact on gravitational physics already. Now the crucial question is at which scale  $k_1 > H_0$  precisely the GR regime ends and the parameters start running.

If we knew the exact RG trajectory we could set up the corresponding RG improved Friedmann equations, interpret the observational data measured in the late Universe within this framework, and deduce  $k_1$  from the redshift of the epoch in which deviations from classical cosmology become visible. In ref. [33] this analysis was performed within the fixed point model but the statistical quality of the presently available data (on high redshift type Ia supernovae) is still too poor to allow for a precise determination of  $k_1$ . It became fairly clear, however, that between  $k = k_1$  and  $k = H_0$  Newton’s constant cannot have changed by more than 1 or 2 orders of magnitude.

Thus we are led to look for possible manifestations of the IR running in gravitationally bound structures which are small on cosmological scales. Clearly the natural place to search for such phenomena are galactic systems. One of their most striking features, as to yet completely unexplained, is the discrepancy between their directly observable mass (due to “luminous matter”) and the mass inferred from the observed motions. This mass discrepancy occurs in all types of galactic systems, from dwarf galaxies to superclusters. Its magnitude ranges from a factor of a few at the kiloparsec scale to a factor of a few hundred at the megaparsec scale [24]. The most popular attempt at explaining this discrepancy is the dark matter hypothesis.

In the present paper we propose that the mass discrepancy is actually not due to the presence of dark matter but rather to the IR renormalization effects. Taking this hypothesis seriously, we shall try to learn something about the RG trajectory by taking advantage of what is known about galaxies. There is a large amount of observational data [25] showing that the orbits of “test particles” moving in typical spiral galaxies

cannot be explained by Newtonian gravity if the gravitational attraction is due to the luminous matter only. Usually the rotation curve  $v(r)$ , the velocity on a circular orbit as a function of the distance to the center, becomes approximately constant for large distances  $r$ , in contradiction to Kepler’s law.

In the following sections we shall demonstrate, by means of an appropriate renormalization group improvement, that such violations of Kepler’s law are exactly what one would expect to occur if  $G(k)$  shows a certain scale dependence at galactic scales already.

A first argument demonstrating that this scenario is not completely unreasonable is the following. A mass discrepancy of a factor of a few hundred at the cluster scale indicates that, very roughly,  $G$  at those scales should not differ from  $G_{\text{lab}}$  by more than a similar factor of a few hundred. This is nicely consistent with what we got for  $G(t_0)/G_{\text{lab}}$  in the fixed point model [33] at somewhat larger scales. Given the many orders of magnitude we are dealing with here this consistency is certainly nontrivial.

A comparatively small ratio  $G_{\text{galaxy}}/G_{\text{lab}}$  of  $\mathcal{O}(10)$  or perhaps  $\mathcal{O}(100)$ , and a similar ratio in cosmology, justifies our earlier use of the linearized flow equation down to  $k = H_0$  which neglects the running between the end of the GR regime and the Hubble scale.

While a renormalization of  $G$  and  $\Lambda$  by a factor of 10 is extremely little compared to the many orders of magnitude their values changed in the UV, it leads to significant modifications of classical Newtonian gravity “in the sky”, at astrophysical scales.

## 4.4 Running $G$ at galactic scales

Henceforth we shall assume that the IR running starts somewhere between solar system and galactic scales.<sup>8</sup> Concentrating on the running of Newton’s constant<sup>9</sup> and, for technical simplicity, spherically symmetric model galaxies, the first step towards their RG improved dynamics is as follows. Given the function  $G = G(k)$  pertaining to the RG trajectory realized in Nature we convert its  $k$ -dependence to a distance dependence by means of an appropriate cutoff identification [30]. As long as curvature effects are small,

---

<sup>8</sup>As for the QCD analogy, a feature of QEG not shared by QCD is the long intermediate classical regime, as a result of which deviations from the  $1/r$ -potential occur near  $k_{\text{term}} \ll m_{\text{P1}}$  only, while in QCD this happens at the scale  $\Lambda_{\text{QCD}}$  which is analogous to  $m_{\text{P1}}$  in other respects.

<sup>9</sup>For small isolated systems such as an individual galaxy the cosmological constant plays no important role probably. (Cosmological effects will be neglected in our discussion of galaxies.)

the obvious choice for spherically symmetric systems is  $k = \xi/r$ , with  $\xi$  a constant of order unity [37]. We define the position dependent Newton constant as

$$G(r) \equiv G(k = \xi/r). \quad (55)$$

By the very construction of the effective average action [12],  $G(r)$  is the parameter which appears in the effective field equations for quantities averaged over a volume of linear dimension  $\approx r$ .

Using  $G(r)$  we can try to RG improve the classical Newton potential  $-G_{\text{lab}}M/r$  by substituting  $G_{\text{lab}} \rightarrow G(r)$ . In the case of the UV renormalization effects [1] it is known that this procedure reproduces the results of the explicit perturbative calculation [40,41]. However, as we shall discuss in the next section the improved action approach predicts a “nonperturbative” large distance correction which is even more important than the one taken into account by replacing  $G_{\text{lab}} \rightarrow G(r)$  in the potential.

The most important question is which  $k$ -dependence we should expect at a typical galactic scale of  $k^{-1} = 1 \text{ kpc} \cdots 100 \text{ kpc}$ , say. As it will turn out, for the trajectory realized in Nature this scale is already outside the domain of validity of the nonlinear Einstein–Hilbert flow equations. Therefore, the best we can do is to make an ansatz for  $G(k)$  which reproduces the “phenomenology” of galaxies as well as possible, and at the same time provides (part of) a natural interpolation between the GR regime and the IR fixed point behavior.

Classical GR is characterized by a vanishing anomalous dimension,  $\eta_N = 0$ . Switching on the renormalization effects, the theoretically simplest option is to assume a nonzero, but constant  $\eta_N$ . Since  $\partial_t G = \eta_N G$  this entails a power law  $G(k) \propto k^{\eta_N}$ . As  $G(k)$  is an increasing function of  $k$ ,  $\eta_N$  is negative. We shall set  $\eta_N = -q$  therefore with a positive constant  $q$ . Thus we tentatively assume that

$$G(k) \propto 1/k^q \quad (56)$$

for the range of  $k$ -values which are relevant to the structure of galaxies. Note that the assumption of an approximately constant  $\eta_N$  is not too restrictive since this range comprises only 2 or 3 orders of magnitude, from 1 kpc and 100 or 1000 kpc, say. The power law (56) leads to the radial dependence

$$G(r) \propto r^q. \quad (57)$$

The consequences of this  $r$ -dependence we are going to explore in a moment. It will lead to phenomenologically acceptable rotation curves if  $q \approx 10^{-6}$ .

There exists an intriguing scenario which would give rise to an approximately constant  $\eta_N$  during some  $k$ -interval in a natural way. Let us assume that, at galactic scales, the RG trajectory approaches a further NGFP, different from the ones discussed above, spends some time in its vicinity, and is finally driven away from it. This fixed point  $(g_*, \lambda_*, \dots)$  must have the  $g$ -coordinate  $g_* = 0$  because then  $\beta_g \equiv (2 + \eta_N) g$  vanishes there without constraining the value of  $\eta_N$ . (Every NGFP with  $g_* \neq 0$  has  $\eta_* = -2$ .) Hence, if  $\eta_* \equiv \eta_N(g_* = 0, \lambda_*, \dots) \equiv -q$  is nonzero, the smallness of the  $\beta$ -functions near the NGFP implies that  $\eta_N(g(k), \lambda(k), \dots)$  is nonzero and approximately  $k$ -independent there.

A fixed point of this kind could only arise within truncations which are much more general than the ones used so far, as the result of a strongly nonperturbative dynamics. (Of course, the perturbative quantization of the Einstein–Hilbert action yields  $\eta_N = 0$  at  $g = 0$ , to all orders.)

The projection of the new fixed point onto the  $g$ - $\lambda$ -plane of Fig. 4 is located exactly on the horizontal ( $g = 0$ ) axis. What makes this scenario particularly plausible is that we know already that the RG trajectory realized in Nature does indeed get extremely close to the  $g = 0$ -axis, as it would be necessary to make  $\eta_N$  approximately  $k$ -independent. However, even if this additional NGFP should not exist as a strict fixed point it is still quite plausible that a behavior similar to (56) can prevail for a short RG time and this is all we need.

## 5 Galaxy rotation curves

In this section we apply the improved-action approach to the problem of the flat galaxy rotation curves. For further details about the general approach we refer to [36], and to [37] for a detailed analysis of spherically symmetric, static “model galaxies”.

The idea is to start from the classical Einstein–Hilbert action  $S_{\text{EH}} = \int d^4x \sqrt{-g} \mathcal{L}_{\text{EH}}$  with the Lagrangian  $\mathcal{L}_{\text{EH}} = (R - 2\Lambda) / (16\pi G)$  and to promote  $G$  and  $\Lambda$  to scalar fields.

This leads to the modified Einstein–Hilbert (mEH) action

$$S_{\text{mEH}}[g, G, \Lambda] = \frac{1}{16\pi} \int d^4x \sqrt{-g} \left\{ \frac{R}{G(x)} - 2 \frac{\Lambda(x)}{G(x)} \right\}. \quad (58)$$

The resulting theory has certain features in common with Brans–Dicke theory; the main difference is that  $G(x)$  (and  $\Lambda(x)$ ) is a prescribed “background field” rather than a Klein–Gordon scalar as usually. Upon adding a matter contribution the action (58) implies the modified Einstein equation<sup>10</sup>

$$G_{\mu\nu} = -\Lambda(x) g_{\mu\nu} + 8\pi G(x) (T_{\mu\nu} + \Delta T_{\mu\nu}). \quad (59)$$

Here  $\Delta T_{\mu\nu}$  is an additional contribution to the energy–momentum tensor due to the  $x$ –dependence of  $G$ :

$$\Delta T_{\mu\nu} \equiv \frac{1}{8\pi} (D_\mu D_\nu - g_{\mu\nu} D^2) \frac{1}{G(x)}. \quad (60)$$

The field equation (59) is mathematically consistent provided  $\Lambda(x)$  and  $G(x)$  satisfy a “consistency condition” which insures that the RHS of (59) has a vanishing covariant divergence.

In ref. [37] we analyzed the weak field, slow–motion approximation of this theory for a time–independent Newton constant  $G = G(\mathbf{x})$  and  $\Lambda \equiv 0$ . In this (modified) Newtonian limit the equation of motion for massive test particles has the usual form,  $\ddot{\mathbf{x}}(t) = -\nabla\phi$ , but the potential  $\phi$  obeys a modified Poisson equation,

$$\nabla^2\phi = 4\pi \bar{G} \rho_{\text{eff}} \quad (61a)$$

with the effective density<sup>11</sup>

$$\rho_{\text{eff}} = \rho + (8\pi \bar{G})^{-1} \nabla^2 \mathcal{N}. \quad (61b)$$

In deriving (61) it was assumed that  $T_{\mu\nu}$  describes pressureless dust of density  $\rho$  and that  $G(\mathbf{x})$  does not differ much from the constant  $\bar{G}$ . We use the parameterization

$$G(\mathbf{x}) = \bar{G} [1 + \mathcal{N}(\mathbf{x})] \quad (62)$$

---

<sup>10</sup>In [36] and [37] a further contribution,  $\theta_{\mu\nu}$ , was added to the energy–momentum tensor in order to describe the 4–momentum of the field  $G(x)$ . Its form is not completely fixed by general principles. But as it does not affect the Newtonian limit [37] we set  $\theta_{\mu\nu} \equiv 0$  here.

<sup>11</sup>In this paper we neglect in  $\rho_{\text{eff}}$  an inessential term  $\mathcal{N} \rho$  relative to  $\rho$ .

and assume that  $\mathcal{N}(\mathbf{x}) \ll 1$ . More precisely, the assumptions leading to the modified Newtonian limit are that the potential  $\phi$ , the function  $\mathcal{N}$ , and typical (squared) velocities  $\mathbf{v}^2$  are much smaller than unity; all terms linear in these quantities are retained, but higher powers ( $\phi^2, \dots$ ) and products of them ( $\phi\mathcal{N}, \dots$ ) are neglected. (In the application to galaxies this is an excellent approximation.) Apart from the rest energy density  $\rho$  of the ordinary (“baryonic”) matter, the effective energy density  $\rho_{\text{eff}}$  contains the “vacuum” contribution

$$(8\pi\overline{G})^{-1}\nabla^2\mathcal{N}(\mathbf{x}) = (8\pi\overline{G}^2)^{-1}\nabla^2G(\mathbf{x}) \quad (63)$$

which is entirely due to the position dependence of Newton’s constant. Since it acts as a source for  $\phi$  on exactly the same footing as  $\rho$  it mimics the presence of “dark matter”.

As the density (63) itself contains a Laplacian  $\nabla^2$ , all solutions of the Newtonian field equation (61) have a very simple structure:

$$\phi(\mathbf{x}) = \widehat{\phi}(\mathbf{x}) + \frac{1}{2}\mathcal{N}(\mathbf{x}). \quad (64)$$

Here  $\widehat{\phi}$  is the solution to the standard Poisson equation  $\nabla^2\widehat{\phi} = 4\pi\overline{G}\rho$  containing only the ordinary matter density  $\rho$ . The simplicity and generality of this result is quite striking.

Up to this point the discussion applies to an arbitrary prescribed position dependence of Newton’s constant, not necessarily related to a RG trajectory. At least in the case of spherically symmetric systems the identification of the relevant geometric cutoff is fairly straightforward,  $k \propto 1/r$ , so that we may consider the function  $G(k)$  as the primary input, implying  $G(r) \equiv G(k = \xi/r)$ . Writing again  $G \equiv \overline{G}[1 + \mathcal{N}]$  we assume that  $G(k)$  is such that  $\mathcal{N} \ll 1$ . Then, to leading order, the potential for a point mass reads, according to (64):

$$\phi(r) = -\frac{\overline{G}M}{r} + \frac{1}{2}\mathcal{N}(r). \quad (65)$$

Several comments are in order here.

**(a)** The reader might have expected to find a term  $-\overline{G}M\mathcal{N}(r)/r$  on the RHS of (65) resulting from Newton’s potential  $\phi_{\text{N}} \equiv -\overline{G}M/r$  by the “improvement”  $\overline{G} \rightarrow G(r)$ . However, this term  $\phi_{\text{N}}\mathcal{N}$  is of second order with respect to the small quantities we are expanding in. In the envisaged application to galaxies, for example,  $\phi_{\text{N}}\mathcal{N}$  is completely negligible compared to the  $\frac{1}{2}\mathcal{N}$ -term in (65).

(b) According to (65), the renormalization effects generate a nonclassical force (per unit test mass) given by  $-\mathcal{N}'(r)/2$  which adds to the classical  $1/r^2$ -term. This force is attractive if  $G(r)$  is an increasing function of  $r$  and  $G(k)$  a decreasing function of  $k$ . This is in accord with the intuitive picture of the antiscreening character of quantum gravity [1]: “Bare” masses get “dressed” by virtual gravitons whose gravitating energy and momentum cannot be shielded and lead to an additional gravitational pull on test masses therefore.

(c) The solution (65) is not an approximation artifact. In [37] we constructed exact solutions of the full nonlinear modified Einstein equations (with  $\mathcal{N}$  not necessarily small) which imply (65) in their respective Newtonian regime. Those exact solutions can be interpreted as a “deformation” of the Schwarzschild metric ( $M \neq 0$ ) or the Minkowski metric ( $M = 0$ ) caused by the position dependence of  $G$ . The solutions related to the Minkowski metric are particularly noteworthy. They contain no ordinary matter (no point mass), but describe a curved spacetime, a kind of gravitational “soliton” which owes its existence entirely to the  $\mathbf{x}$ -dependence of  $G$ . At the level of eq. (65) they correspond to the  $M = 0$ -potential  $\phi = \frac{1}{2}\mathcal{N}$  which solves the modified Poisson equation if the contribution  $\propto \nabla^2\mathcal{N}$  is the only source term. In the picture where dark matter is replaced with a running of  $G$  this solution corresponds to a pure dark matter halo containing no baryonic matter (yet). The fully relativistic  $M = 0$ -solutions might be important in the early stages of structure formation [37].

Let us make a simple model of a spherically symmetric “galaxy”. For an arbitrary density profile  $\rho = \rho(r)$  the solution of eq. (61) reads

$$\phi(r) = \int_0^r dr' \frac{\overline{G} \mathcal{M}(r')}{r'^2} + \frac{1}{2} \mathcal{N}(r) \quad (66)$$

where  $\mathcal{M}(r) \equiv 4\pi \int_0^r dr' r'^2 \rho(r')$  is the mass of the ordinary matter contained in a ball of radius  $r$ . We are interested in periodic, circular orbits of test particles in the potential (66). Their velocity is given by  $v^2(r) = r \phi'(r)$  so that we obtain the rotation curve

$$v^2(r) = \frac{\overline{G} \mathcal{M}(r)}{r} + \frac{1}{2} r \frac{d}{dr} \mathcal{N}(r). \quad (67)$$

We identify  $\rho$  with the density of the ordinary luminous matter and model the luminous core of the galaxy by a ball of radius  $r_0$ . The mass of the ordinary matter

contained in the core is  $\mathcal{M}(r_0) \equiv \mathcal{M}_0$ , the “bare” total mass of the galaxy. Since, by assumption,  $\rho = 0$  and hence  $\mathcal{M}(r) = \mathcal{M}_0$  for  $r > r_0$ , the potential outside the core is  $\phi(r) = -\overline{G} \mathcal{M}_0/r + \mathcal{N}(r)/2$ . We refer to the region  $r > r_0$  as the “halo” of the model galaxy.

As an example, let us adopt the power law  $G(k) \propto k^{-q}$  which we motivated in Section 4. We assume that this  $k$ -dependence starts inside the core of the galaxy (at  $r < r_0$ ) so that  $G(r) \propto r^q$  everywhere in the halo. For the modified Newtonian limit to be realized, the position dependence of  $G$  must be weak. Therefore we shall tentatively assume that the exponent  $q$  is very small ( $0 < q \ll 1$ ); applying the model to real galaxies this will turn out to be the case actually. Thus, expanding to first order in  $q$ ,  $r^q = 1 + q \ln(r) + \dots$ , we obtain  $G(r) = \overline{G} [1 + \mathcal{N}(r)]$  with

$$\mathcal{N}(r) = q \ln(\kappa r) \tag{68}$$

where  $\kappa$  is a constant. In principle the point  $\overline{G}$  about which we linearize is arbitrary, but in the present context  $\overline{G} \equiv G_{\text{lab}}$  is the natural choice. In the halo, eq. (68) leads to a logarithmic modification of Newton’s potential

$$\phi(r) = -\frac{\overline{G} \mathcal{M}_0}{r} + \frac{q}{2} \ln(\kappa r). \tag{69}$$

The corresponding rotation curve is

$$v^2(r) = \frac{\overline{G} \mathcal{M}_0}{r} + \frac{q}{2}. \tag{70}$$

Remarkably, at large distances  $r \rightarrow \infty$  the velocity approaches a constant  $v_\infty = \sqrt{q/2}$ . Obviously the rotation curve implied by the  $k^{-q}$ -trajectory does indeed become flat at large distances – very much like those we observe in Nature.

Typical measured values of  $v_\infty$  range from 100 to 300 km/sec so that, in units of the speed of light,  $v_\infty \approx 10^{-3}$ . Thus, ignoring factors of order unity for a first estimate, we find that the data require an exponent of the order

$$q \approx 10^{-6}. \tag{71}$$

The smallness of this number justifies the linearization with respect to  $\mathcal{N}$ . It also implies that the variation of  $G$  inside a galaxy is extremely small. The relative variation of

Newton's constant from some  $r_1$  to  $r_2 > r_1$  is  $\Delta G/G = q \ln(r_2/r_1)$ . As the radial extension of a halo comprises only 2 or 3 orders of magnitude the variation between the inner and the outer boundary of the halo is of the order  $\Delta G/G \approx q$ , i. e. Newton's constant changes by one part in a million only.

Including the core region, the complete rotation curve reads

$$v^2(r) = \frac{\overline{G} \mathcal{M}(r)}{r} + \frac{q}{2}. \quad (72)$$

The  $r$ -dependence of this velocity is in qualitative agreement with the observations. For realistic density profiles,  $\mathcal{M}(r)/r$  is an increasing function for  $r < r_0$ , and it decays as  $\mathcal{M}_0/r$  for  $r > r_0$ . As a result,  $v^2(r)$  rises steeply at small  $r$ , then levels off, goes through a maximum at the boundary of the core, and finally approaches the plateau from above. Some galaxies indeed show a maximum after the steep rise, but typically it is not very pronounced, or is not visible at all. The prediction of (70) for the characteristic  $r$ -scale where the plateau starts is  $2\overline{G} \mathcal{M}_0/q$ ; at this radius the classical term  $\overline{G} \mathcal{M}_0/r$  and the nonclassical one,  $q/2$ , are exactly equal. With  $q = 10^{-6}$  and  $\mathcal{M}_0 = 10^{11} M_\odot$  one obtains 9 kpc, which is just the right order of magnitude.

The above  $v^2(r)$  is identical to the one obtained from standard Newtonian gravity by postulating dark matter with a density  $\rho_{\text{DM}} \propto 1/r^2$ . We see that if  $G(k) \propto k^{-q}$  with  $q \approx 10^{-6}$  no dark matter is needed. The resulting position dependence of  $G$  leads to an effective density  $\rho_{\text{eff}} = \rho + q/(8\pi \overline{G} r^2)$  where the  $1/r^2$ -term, well known to be the source of a logarithmic potential, is present as an automatic consequence of the RG improved gravitational dynamics.

We consider these results a very encouraging and promising indication pointing in the direction that quantum gravitational renormalization effects could be the origin of the plateaus in the observed galaxy rotation curves. If so, the underlying RG trajectory of QEG is characterized by an almost constant anomalous dimension  $\eta_N = -q \approx -10^{-6}$  for  $k$  in the range of galactic scales.

Is the Einstein–Hilbert truncation sufficient to search for this trajectory? Unfortunately the answer is no. According to eq. (10c),  $\eta_N$  is proportional to  $g$  which is extremely tiny in the regime of interest, smaller than its solar system value  $10^{-92}$ . In order to achieve a  $|\eta_N|$  as large as  $10^{-6}$ , the smallness of  $g$  must be compensated by large IR enhancement factors. As a result,  $\lambda$  should be extremely close to  $1/2$ , in which case the RHS of (10c)

is dominated by the pole term:  $\eta_N \approx -(6g/\pi)(1-2\lambda)^{-1}$ . Assuming  $g \approx 10^{-92}$  as a rough estimate, a  $q$ -value of  $10^{-6}$  would require  $1-2\lambda \approx 10^{-86}$ . It is clear that when  $1-2\lambda$  is so small the Einstein–Hilbert trajectory is by far too close to its termination point to be a reliable approximation of the true one. Moreover,  $\eta_N(g(k), \lambda(k))$  is not approximately  $k$ -independent in this regime. Thus we must conclude that an improved truncation will be needed for an investigation of the conjectured RG behavior at galactic scales, in particular to search for the  $g_* = 0$ -fixed point speculated about at the end of Section 4.

It is clear that the above model of a galaxy is still quite simplistic and does not yet reproduce all phenomenological aspects of the mass, size, and angular momentum dependence of the rotation curves for different galactic systems. In particular  $v_\infty$  is a universal constant here and does not obey the empirical Tully–Fisher relation. As we explained in [37] to which the reader is referred for further details these limitations are due to the calculational scheme used here (“cutoff identification”, etc.). Usually this scheme can provide a first qualitative or semi-quantitative understanding, but if one wants to go beyond this first approximation, a full fledged calculation of  $\Gamma[g_{\mu\nu}]$  would be necessary which is well beyond our present technical possibilities.

## 6 Summary and conclusion

In this paper we assumed that Quantum Einstein Gravity correctly describes gravity on all length scales and tried to identify the underlying RG trajectory realized in Nature. Along this trajectory, we found a regime where the running of the gravitational parameters is unmeasurably small, the domain of classical General Relativity. The renormalization effects become strong both at momentum scales  $k$  much larger (UV regime) and much smaller (IR regime) than those of the GR regime. In the UV regime, for  $k \rightarrow \infty$ , the trajectory approaches a non-Gaussian fixed point. By definition, QEG is the “asymptotically safe” theory whose bare action equals the fixed point action, guaranteeing its nonperturbative renormalizability. We analyzed a potential IR divergence (instability) in the flow equation which occurs in the Einstein–Hilbert truncation already, and we argued that it triggers significant renormalization effects in the IR, i.e. at distances larger than those where classical GR was successfully tested. In particular, Newton’s constant increases for

decreasing  $k$  so that  $G$  should appear to be larger at galactic or cosmological scales than in a terrestrial or solar system “laboratory”. Looking for possible manifestations of this effect we analyzed the possibility that the almost flat plateaus observed in the rotation curves of spiral galaxies, usually attributed to the presence of dark matter, are actually due to the RG running of Newton’s constant. While the galactic regime is inaccessible with the Einstein–Hilbert truncation, a phenomenological analysis in the framework of the improved action approach revealed that a power law–type scale dependence  $G(k) \propto k^{-q}$ , corresponding to an (approximately) constant anomalous dimension  $\eta_N$ , leads to rotation curves which are in qualitative agreement with those found in Nature. In particular they become perfectly flat at sufficiently large distances.

As a by–product we arrived at a new understanding of the cosmological constant problem: By analyzing the RG trajectories among which Nature could have chosen we saw that there exist no trajectories which, at the same time, would predict a long classical regime and a large cosmological constant. If there is a Universe inhabited by human beings who manage to verify that gravity behaves according to classical General Relativity over many different length scales, they unavoidably will observe a cosmological constant which is extremely small compared to the value of  $1/G \equiv m_{\text{Pl}}^2$  they measure. Conversely, if  $\Lambda$  is not small, it is also not constant, so GR is not valid, and there is no point wondering about the value of a non–constant “constant”. This argument does not seem to require a detailed understanding of the IR effects since the data indicate that in our world, between the end of the GR regime and the Hubble scale,  $G$  and  $\Lambda$  changed by comparatively small factors only.

As for the IR effects, it will be exciting to see whether the properties of the RG trajectory of QEG which we predicted can be confirmed by more advanced ab initio calculations. Clearly more general truncations for the effective average action, involving nonlocal invariants for instance, should be explored for this purpose. In view of recent progress [18] made on causal (Lorentzian) dynamical triangulations [17] one also may hope that at some point it will be possible to make contact with numerical simulations. This could lead to an independent confirmation of the picture we have drawn in the present paper.

Acknowledgement: We would like to thank A. Bonanno, O. Lauscher, R. Loll, F. Saueressig, and J. Smit for helpful discussions.

## References

- [1] M. Reuter, Phys. Rev. D 57 (1998) 971 and hep-th/9605030.
- [2] D. Dou and R. Percacci, Class. Quant. Grav. 15 (1998) 3449.
- [3] O. Lauscher and M. Reuter, Phys. Rev. D 65 (2002) 025013 and hep-th/0108040.
- [4] M. Reuter and F. Saueressig, Phys. Rev. D 65 (2002) 065016 and hep-th/0110054.
- [5] O. Lauscher and M. Reuter, Class. Quant. Grav. 19 (2002) 483 and hep-th/0110021;  
Phys. Rev. D 66 (2002) 025026 and hep-th/0205062;  
Int. J. Mod. Phys. A 17 (2002) 993 and hep-th/0112089.
- [6] W. Souma, Prog. Theor. Phys. 102 (1999) 181.
- [7] R. Percacci and D. Perini, Phys. Rev. D 67 (2003) 081503; Phys. Rev. D 68 (2003) 044018;  
D. Perini, Nucl. Phys. Proc. Suppl. 127 C (2004) 185;  
R. Percacci and D. Perini, preprint hep-th/0401071.
- [8] M. Reuter and F. Saueressig, Phys. Rev. D 66 (2002) 125001 and hep-th/0206145;  
Fortschr. Phys. 52 (2004) 650 and hep-th/0311056.
- [9] D. Litim, Phys. Rev. Lett. 92 (2004) 201301.
- [10] S. Weinberg in *General Relativity, an Einstein Centenary Survey*, S.W. Hawking and W. Israel (Eds.), Cambridge University Press (1979); S. Weinberg, hep-th/9702027.
- [11] C. Wetterich, Phys. Lett. B 301 (1993) 90.
- [12] For a review see: J. Berges, N. Tetradis and C. Wetterich, Phys. Rep. 363 (2002) 223; C. Wetterich, Int. J. Mod. Phys. A 16 (2001) 1951.
- [13] M. Reuter and C. Wetterich, Nucl. Phys. B 417 (1994) 181, Nucl. Phys. B 427 (1994) 291, Nucl. Phys. B 391 (1993) 147, Nucl. Phys. B 408 (1993) 91;  
M. Reuter, Phys. Rev. D 53 (1996) 4430, Mod. Phys. Lett. A 12 (1997) 2777.

- [14] P. Forgács and M. Niedermaier, hep-th/0207028;  
M. Niedermaier, JHEP 12 (2002) 066; Nucl. Phys. B 673 (2003) 131.
- [15] M. Reuter and C. Wetterich, Phys. Rev. D 56 (1997) 7893;  
H. Gies, Phys. Rev. D 66 (2002) 025006.
- [16] O. Lauscher, M. Reuter and C. Wetterich, Phys. Rev. D 62 (2000) 125021  
and hep-th/0006099.
- [17] A. Dasgupta and R. Loll, Nucl. Phys. B 606 (2001) 357;  
J. Ambjørn, J. Jurkiewicz and R. Loll, Nucl. Phys. B 610 (2001) 347;  
R. Loll, Nucl. Phys. Proc. Suppl. 94 (2001) 96;  
J. Ambjørn, gr-qc/0201028.
- [18] J. Ambjørn, J. Jurkiewicz and R. Loll, preprint hep-th/0404156.
- [19] See, for instance, M. Böhm, A. Denner and H. Joos, *Gauge Theories of the Strong and Electroweak Interaction*, Teubner, Stuttgart, 2001.
- [20] N.C. Tsamis and R.P. Woodard, Phys. Lett. B 301 (1993) 351; Ann. Phys. 238 (1995) 1;  
Nucl. Phys. B 474 (1996) 235.
- [21] I. Antoniadis and E. Mottola, Phys. Rev. D 45 (1992) 2013.
- [22] O. Bertolami, J.M. Mourão and J. Pérez–Mercader, Phys. Lett. B 311 (1993) 27;  
O. Bertolami and J. Garcia–Bellido, Int. J. Mod. Phys. D 5 (1996) 363;  
T. Goldman, J. Pérez–Mercader, F. Cooper and M. Martin Nieto, Phys. Lett. B 281 (1992) 219.
- [23] O. Bertolami and J. Garcia–Bellido, Nucl. Phys. Proc. Suppl. 48 (1996) 122.
- [24] See, for instance, T. Padmanabhan, *Theoretical Astrophysics*, Vol. 3, Cambridge University Press, 2002.
- [25] See, for instance, F. Combes, P. Boissé, A. Mazure and A. Blanchard, *Galaxies and Cosmology*, Springer, New York, 2002.

- [26] M. Milgrom, *Astrophys. J.* 270 (1983) 371; 270 (1983) 384; 270 (1983) 365;  
M. Milgrom in *Dark matter in astrophysics and particle physics*, H.V. Klapdor–Kleingrothaus and L. Baudis (Eds.), Heidelberg, 1998; *Acta Phys. Polon. B* 32 (2001) 3613.
- [27] P.D. Mannheim and D. Kazanas, *Astrophys. J.* 342 (1989) 635;  
P.D. Mannheim and J. Kmetko, preprint astro-ph/9602094;  
P.D. Mannheim, *Astrophys. J.* 479 (1997) 659.
- [28] A. Aguirre, C.P. Burgess, A. Friedland and D. Nolte,  
*Class. Quant. Grav.* 18 (2001) R 223.
- [29] C. Wetterich, *Phys. Lett. B* 522 (2001) 5.
- [30] A. Bonanno and M. Reuter, *Phys. Rev. D* 62 (2000) 043008 and hep-th/0002196;  
*Phys. Rev. D* 60 (1999) 084011 and gr-qc/9811026.
- [31] A. Bonanno and M. Reuter, *Phys. Rev. D* 65 (2002) 043508 and hep-th/0106133.
- [32] A. Bonanno and M. Reuter, *Phys. Lett. B* 527 (2002) 9 and astro-ph/0106468;  
*Int. J. Mod. Phys. D* 13 (2004) 107 and astro-ph/0210472.
- [33] E. Bentivegna, A. Bonanno and M. Reuter, *JCAP* 01 (2004) 001  
and astro-ph/0303150.
- [34] A. Bonanno, G. Esposito and C. Rubano, *Gen. Rel. Grav.* 35 (2003) 1899;  
preprint gr-qc/0403115.
- [35] T. Tsuneyama, preprint hep-th/0401110.
- [36] M. Reuter and H. Weyer, *Phys. Rev. D* 69 (2004) 104022 and hep-th/0311196.
- [37] M. Reuter and H. Weyer, MZ-TH/04-14, to appear in *Phys. Rev. D*.
- [38] C. Wetterich, *Gen. Rel. Grav.* 30 (1998) 159.
- [39] S. Weinberg, *Rev. Mod. Phys.* 61 (1989) 1;  
M. Reuter and C. Wetterich, *Phys. Lett. B* 188 (1987) 38.

- [40] J.F. Donoghue, Phys. Rev. Lett. 72 (1994) 2996; Phys. Rev. D 50 (1994) 3874.
- [41] N.E.J. Bjerrum–Bohr, Phys. Rev. D 66 (2002) 084023;  
N.E.J. Bjerrum–Bohr, J.F. Donoghue and B.R. Holstein, Phys. Rev. D 67 (2003) 084033, Phys. Rev. D 68 (2003) 084005.